

Spatial and isotopic niche partitioning during winter in chinstrap and Adélie penguins from the South Shetland Islands

JEFFERSON T. HINKE,^{1,†} MICHAEL J. POLITO,^{2,3} MICHAEL E. GOEBEL,¹ SHARON JARVIS,⁴ CHRISTIAN S. REISS,¹
SIMON R. THORROLD,³ WAYNE Z. TRIVELPIECE,¹ AND GEORGE M. WATTERS¹

¹Antarctic Ecosystem Research Division, Southwest Fisheries Science Center, National Marine Fisheries Service, National Oceanic and Atmospheric Administration, La Jolla, California 92037 USA

²Department of Oceanography and Coastal Sciences, Louisiana State University, Baton Rouge, Louisiana 70803 USA

³Biology Department, Woods Hole Oceanographic Institution, Woods Hole, Massachusetts 02543 USA

⁴Aviculture Department, SeaWorld, Orlando, Florida 32821 USA

Citation: Hinke, J. T., M. J. Polito, M. E. Goebel, S. Jarvis, C. S. Reiss, S. R. Thorrold, W. Z. Trivelpiece, and G. M. Watters. 2015. Spatial and isotopic niche partitioning during winter in chinstrap and Adélie penguins from the South Shetland Islands. *Ecosphere* 6(7):125. <http://dx.doi.org/10.1890/ES14-00287.1>

Abstract. Closely related species with similar ecological requirements should exhibit segregation along spatial, temporal, or trophic niche axes to limit the degree of competitive overlap. For migratory marine organisms like seabirds, assessing such overlap during the non-breeding period is difficult because of long-distance dispersal to potentially diffuse foraging habitats. Miniaturization of geolocation devices and advances in stable isotope analysis (SIA), however, provide a robust toolset to quantitatively track the movements and foraging niches of wide ranging marine animals throughout much of their annual cycle. We used light-based geolocation tags and analyzed stable carbon and nitrogen isotopes from tail feathers to simultaneously characterize winter movements, habitat utilization, and overlap of spatial and isotopic niches of migratory chinstrap (*Pygoscelis antarctica*) and Adélie (*P. adeliae*) penguins during the austral winter of 2012. Chinstrap penguins exhibited a higher diversity of movements and occupied portions of the Southern Ocean from 138° W to 30° W within a narrow latitudinal band centered on 60° S. In contrast, all tracked Adélie penguins exhibited smaller-scale movements into the Weddell Sea and then generally along a counter-clockwise path as winter advanced. Inter-specific overlap during the non-breeding season was low except during the months immediately adjacent to the summer breeding season. Intra-specific overlap by chinstraps from adjacent breeding colonies was higher throughout the winter. Spatial segregation appears to be the primary mechanism to maintain inter- and intra-specific niche separation during the non-breeding season for chinstrap and Adélie penguins. Despite low spatial overlap, however, the data do suggest that a narrow pelagic corridor in the southern Scotia Sea hosted both chinstrap and Adélie penguins for most months of the year. Shared occupancy and similar isotopic signatures of the penguins in that region suggests that the potential for inter-specific competition persists during the winter months. Finally, we note that SIA was able to discriminate eastward versus westward migrations in penguins, suggesting that SIA of tail feathers may provide useful information on population-level distribution patterns for future studies.

Key words: Antarctica; geolocation; migration; niche; *Pygoscelis adeliae*; *Pygoscelis antarctica*; stable isotope; winter.

Received 8 September 2014; revised 2 March 2015; accepted 3 April 2015; final version received 6 May 2015; **published** 29 July 2015. Corresponding Editor: B. Maslo.

Copyright: © 2015 Hinke et al. This is an open-access article distributed under the terms of the Creative Commons Attribution License, which permits unrestricted use, distribution, and reproduction in any medium, provided the original author and source are credited. <http://creativecommons.org/licenses/by/3.0/>

† **E-mail:** Jefferson.Hinke@noaa.gov

INTRODUCTION

Ecological theory predicts that closely related species with similar ecological requirements should exhibit niche partitioning to limit the degree of competitive overlap where they co-occur (Ricklefs and Miller 1999). For example, because many sympatric colonial seabird assemblages have restricted foraging ranges during the breeding season they are often used as model assemblages to study mechanisms of inter-specific and intra-specific niche partitioning in environments with limited resources (Lewis et al. 2001, Wilson 2010). These studies have shown that competitive overlap may be reduced among sympatric competitors via segregation along the trophic axes of species' respective foraging niches (e.g., relying on different food resources; Croxall et al. 1997, Cherel et al. 2008). In addition, segregation in spatial (e.g., vertical or horizontal displacement) and temporal (e.g., shifts in peak resource or habitat use) niche axes can also effectively reduce competition between breeding seabirds (Wilson 2010, Connan et al. 2014). Foraging niche segregation is also evident between neighboring populations of the same species as the potential for intra-specific competition is often higher than competition among congeners (Masello et al. 2010).

Most studies on the foraging niches of seabirds have focused on the breeding season because of ease of access to study animals and the expectation that competition during the breeding season is exacerbated by the increased demands of raising offspring and the constraints of central place foraging. Studies examining foraging ecology during the non-breeding periods are less common, despite recognition that foraging grounds during the non-breeding period may contain high densities of competitors (e.g., Karnovsky et al. 2007). The miniaturization of animal-borne loggers has significantly improved the ability to track the long-distance movements of seabirds during the non-breeding season (e.g., Kooyman et al. 2000, Clarke et al. 2003, Bost et al. 2004, Shaffer et al. 2006, Quillfeldt et al. 2012). In addition, advances in the use of stable isotope analysis (SIA), which is based on the principle that animals “are what and where they eat” (Inger and Bearhop 2008, Bond and Jones 2009), now provide the ability to estimate foraging

niches from tissues grown during the non-breeding period when individuals are away from land (e.g., Polito et al. 2011a). In combination, direct tracking and SIA provide a robust toolset to quantitatively track the movements and foraging niches of wide-ranging marine organisms, including seabirds, throughout much of their annual cycle (González-Solís et al. 2007, Block et al. 2011, Polito et al. 2011a, Seminoff et al. 2012). Interestingly, recent studies using the approaches above have noted clear patterns of spatial and temporal foraging niche segregation within and between sympatric seabird species during the winter months when they are away from breeding colonies (Thiebot et al. 2011, Ratcliffe et al. 2014). These results suggest that some seabird assemblages have evolved behavioral mechanisms that help to limit inter and intra-specific competitive overlap during the non-breeding period.

In this study we focus on the movements of chinstrap (*Pygoscelis antarctica*) and Adélie (*P. adeliae*) penguins during the non-breeding season (March–October; hereafter “winter” unless otherwise specified). Both species exhibit population declines in the Antarctic Peninsula region in response to climate warming, consequent loss of sea ice, and reductions in the availability of Antarctic krill (*Euphausia superba*; Trivelpiece et al. 2011, Lynch et al. 2012). Habitat availability and foraging conditions encountered during winter may be important drivers of the observed changes in penguin abundance in the Antarctic Peninsula region (Hinke et al. 2007), further suggesting the need to examine dispersal routes and foraging habitats of these species during winter. A constraint of such monitoring, however, is that Adélie and chinstrap penguins exhibit seasonal migrations between summer breeding sites and winter foraging habitats that may be separated by hundreds or thousands of kilometers (Wilson et al. 1998, Clarke et al. 2003, Trivelpiece et al. 2007, Ballard et al. 2010, Biuw et al. 2010). Accordingly, direct comparisons of marine habitat use and foraging niches of these sympatric competitors during the non-breeding season remain an important gap in our understanding of Adélie and chinstrap penguin ecology.

On a broad-scale, ship-based observations suggest that these two species may segregate

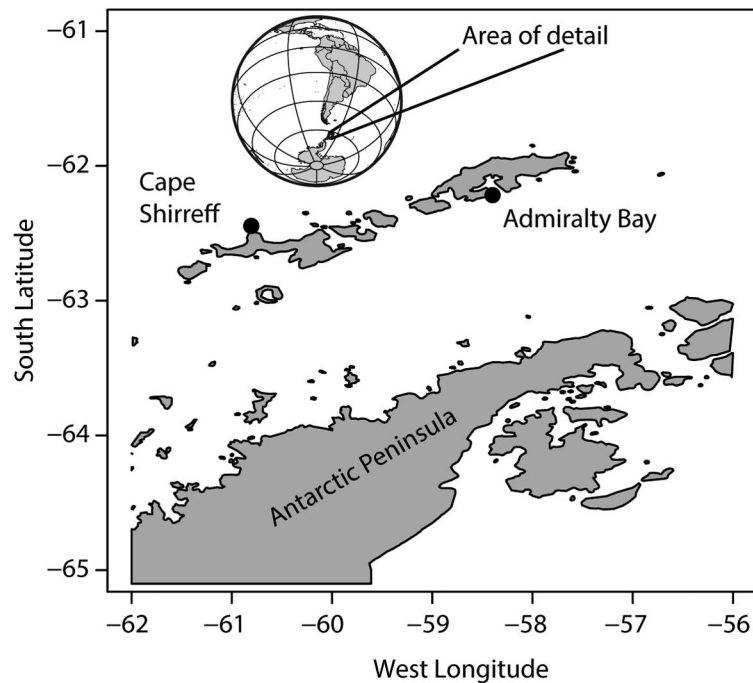


Fig. 1. Study area and location of tagging sites, indicated by black dots, at Cape Shirreff, Livingston Island and Admiralty Bay, King George Island, South Shetland Islands, Antarctica.

winter foraging areas based on the presence of sea ice. Adélie penguins are typically observed in marginal ice zones while chinstrap penguins often are observed in open waters north of the ice edge (Ainley et al. 1994). Winter tracking studies have confirmed seasonal occupancy of ice zones for Adélie penguins (Clarke et al. 2003, Ballard et al. 2010, Dunn et al. 2011, Erdmann et al. 2011) while chinstrap penguins tend to be in areas typically free of ice (Wilson et al. 1998, Trivelpiece et al. 2007, Biuw et al. 2010). Even so, the previous tracking studies have examined the winter movements of each species in isolation. Consequently addressing spatial segregation during the non-breeding season has been hampered by low sample sizes and a lack of temporal (year of study) and spatial (breeding population examined) overlap between studies.

Here we report on research to simultaneously track individuals from two breeding colonies of Adélie and chinstrap penguins in the South Shetland Islands, Antarctic Peninsula with archival geolocation tags and examine foraging niche space using SIA. Our goals are to assess the degree and mechanism (spatial, temporal and/or

trophic) of foraging niche partitioning that occurs during the non-breeding periods, both between these two species from the same breeding colony in Admiralty Bay, King George Island, as well as between members of the same species (chinstrap penguins) from Admiralty Bay and Cape Shirreff, Livingston Island; these colonies are separated by 120 km (Fig. 1). We predict that spatial segregation of foraging areas will occur between species based on previously observations of differences in foraging areas evident during the breeding period (Wilson 2010) and winter observations that indicate Adélie penguins are more commonly observed in marginal ice zones while chinstrap penguins occupy open waters north of the ice edge (Ainley et al. 1994). Because neighboring populations of con-specifics likely occupy the same ecological niche, we predict that chinstrap penguins from different colonies will exhibit relatively higher overlap in winter foraging areas and isotopic niche space, as intra-specific segregation would be expected to occur within a shared habitat rather than occupation of distinct habitats (Thiebot et al. 2011, Thiebot et al. 2012, but see Ratcliffe et al. 2014).

Table 1. Summary information on number of deployments, recoveries, and data collection from GLS tags, including mean and range of deployment durations.

Tagging locale	Species	No. tags			No. tags used for analysis		Duration of deployments (d)	
		Deployed	Recovered	Downloaded	Winter habitat	Isotope period [†]	Mean	Range
Admiralty Bay	Adélie	51	36	34	29	19	211	32–423
Admiralty Bay	Chinstrap	50	30	20	19	16	141	23–290
Cape Shirreff	Chinstrap	61	46	37	34	21	121	30–313

[†] Tag failures prior to the isotope study period, assumed to be 40–100 days after molt initiation, reduced the sample sizes of tags during of the isotope period relative to those used for habitat mapping.

METHODS

Tagging

Chinstrap and Adélie penguins from Cape Shirreff, Livingston Island (62.46° S, 60.79° W) and Admiralty Bay, King George Island (62.21° S, 58.42° W; Fig. 1) were captured during the 2011/12 breeding season (Table 1) and fitted with Lotek Nano-Lat 2900-series archival geolocation tags (hereafter GLS; Lotek Wireless, St. Johns, Newfoundland, Canada) to monitor dispersal and habitat utilization. Tagging was concentrated in one small sub-colony for each species at each site to help minimize search effort and maximize recovery rates in the following spring. The GLS tags were affixed to a white plastic ring band with two small plastic cable wraps and the ring band was then fitted to the right tarsus of each bird. Each GLS tag had dimensions 8 × 15 × 7 mm and weighed 2 g in air. The tags provided daily estimates of latitude, longitude, and surface temperature.

Effects of tags

The attachment of external archival tags to seabirds is a common practice among field research programs. Miniaturization of tags and the ability to use tarsus bands for attachment are critical for eliminating damage to the plumage by adhesives. Based on observations in the field, we note that the attachment method, similar to that of Ballard et al. (2010), and the size of the tag used in this study appeared to have had minor impacts on our study penguins. The observed return rate, roughly 70% (Table 1), was consistent with expected returns given mortality rates for Pygoscelid penguins in the region (Hinke et al. 2014). Observers in the field confirmed that no birds presented serious injury and exhibited only minor callusing from over 10 months of wear.

Observers also confirmed normal breeding behaviors and successful breeding attempts among many tracked birds. We note, however, that no effort was made to identifiably mark or further disturb the birds once the GLS tag was removed and the tail feather collected. We therefore assume the impacts of tagging were minor and had no significant bias on the large-scale tracking or stable isotope data collected.

Bias and error in location

To estimate bias and error in position estimates from the GLS tags, we used data from four GLS control tags that were either fixed-position deployments at Cape Shirreff ($N = 2$) or animal-borne deployments ($N = 2$) with simultaneous ARGOS-based satellite estimates of position that served as mobile controls. The estimation procedure for the bias correction and location error in the GLS data is provided in Appendix A. Preliminary analysis of the control-tag data indicated bias in location was present, particularly for latitude estimates during mid-winter months. We therefore used the control-tag data to estimate weekly bias corrections for correcting raw data from tracked animals, and we estimated weekly errors in the control-tag data for input into modeling penguin movement tracks (see *Materials and methods: Habitat utilization*). All data from the tagged penguins were bias-corrected and then filtered with a speed filter (Freitas et al. 2008), assuming maximum sustained swim speeds of 2 m·s⁻¹, to remove anomalous data points prior to further analyses.

Habitat utilization

Habitat utilization, defined here as the proportion of time spent in a specified grid cell for each month, was estimated via a four-step process. First, we fitted a state-space model

(Johnson et al. 2008) to the bias-corrected data from each tag to produce hourly estimates of probable location. The model was fitted using the R (R Core Team 2012) package ‘crawl’ (Johnson et al. 2008). As an error structure for the model, we used the weekly estimates of location error as described in detail in the Appendix A. Second, based on the parameters of the fitted model, we generated 100 alternative track lines, with position estimates for each hour, for all tags. The set of alternative track lines was generated to account for the uncertainty in individual location estimates, and we assumed that the set of 100 provided a sufficient sample to characterize uncertainty in habitat use. Third, we aggregated the 100 probable track lines from all individuals and split the dataset into monthly components. The monthly temporal resolution reported here is arbitrary, but we felt that this scale best integrated across the movement rates and position errors while providing sufficient temporal resolution to identify movement patterns on a large scale (e.g., Thiebot et al. 2011). Finally, we overlaid the aggregated monthly data onto a grid to estimate the proportion of time spent in any grid cell. For this analysis, we used a grid-cell size of 3° longitude by 2° latitude based on the maximum location error in the control-tag data (Appendix A). We note that the relatively large size of this grid cell precludes fine-scale differentiation of habitat use; for example, sea ice could provide a natural boundary separating Adélie and chinstrap penguins in a particular grid cell. However, we assume that shared occupancy of a particular grid cell is indicative of the importance of that general area to all individuals and will hereafter refer to that shared occupancy of the grid cell as overlap in habitat use. With this caveat and broad-scale frame of reference, we do not focus on individual migratory routes or movement rates but prefer a more probabilistic approach to identify frequently occupied areas based on likely positions given the uncertain raw estimates of position. We also limit our discussion of basin-scale movements to an arbitrary monthly time frame to align the large spatial scale with a relatively long-term temporal scale of resolution.

We used the simple overlap index of Schoener (1970) to quantify the degree of inter-specific (chinstrap versus Adélie penguin) and intra-specific (chinstrap penguins from Cape Shirreff

and Admiralty Bay) habitat overlap, where a value of one indicates identical occupancy of grid cells for the two groups being compared, while a value of zero indicates the absence of overlap. We calculated the overlap index for each month using two different metrics of habitat utilization. First, we calculated a “spatial” overlap index based on the proportion of time spent in each grid cell. This calculation measured the extent of shared occupancy of grid cells during the time period of interest. The second index measured overlap on an “individual” basis by calculating the proportion of individuals from the tagged sample of each species that occupied each grid cell during the time period of interest.

Environmental covariates

Sea ice is a critical component of marine habitat in the Southern Ocean. After the breeding season Adélie penguins typically molt and forage in concentrated pack ice (50–80%; Ballard et al. 2010, Dunn et al. 2011), while chinstrap penguins are generally observed north of the sea-ice edge in open water (Ainley et al. 1994). Therefore, these species would be expected to track the advance and retreat of sea ice. We used mean monthly sea-ice concentration data for 2012, reported on a 0.25° latitude-longitude grid, available from the National Snow and Ice Data Center (<http://nsidc.org/data/polaris/>), to estimate the extent of sea ice throughout the range of marine habitats used by the tagged penguins. We used contours of 15% and 50% sea-ice concentrations to compare with the spatial distributions of tagged individuals. The 15% contour represents an effective ice edge and the 50% contour was chosen as a northern limit for Adélie penguin. We hypothesized that chinstrap penguins would occupy marine habitats mainly north of the 15% sea-ice concentration margin, while Adélie penguins would occupy habitats mainly south of 50% sea-ice concentration margin. Finally, we used sea-surface temperature data (Reynolds et al. 2002) for 2012, provided on a 1° latitude-longitude grid by the Earth System Research Laboratory (<http://www.esrl.noaa.gov/psd/>) and daily estimates of surface temperatures recorded by the GLS tags to identify broad-scale thermal ranges used by the tagged penguins. For plotting, all isotherms and ice contours were smoothed using a loess smoother.

Tail-feather sampling

A single, central tail feather was plucked from all birds that were recaptured with a GLS tag to assess penguin foraging ecology during winter using SIA. Feathers are metabolically inert following synthesis and therefore encapsulate an isotopic record of avian diets and foraging habitat use from when and where they were grown (Hobson 1999, Ramos and González-Solís 2012). Therefore, we used data on the timing and rate of growth of tail feathers from a captive study, detailed in Appendix B, of Adélie penguins to select a 0.5-cm section from the shaft of each tail feather from GLS tracked individuals that was grown approximately 59 ± 11 and 69 ± 20 days following the onset of molt for chinstrap and Adélie penguins, respectively. Given uncertainty in growth rates of tail feathers in the wild, isotopic turnover rates in feathers (see *Discussion*), and error in estimates of position from the tracking data (Appendix A), we used a more conservative 95% confidence interval range of 40–100 days (Appendix B) following the onset of molt to compare the isotopic composition of tail feathers with the spatial distribution of animals. Thus, the section of tail feather used for SIA reflects a growth period from late March to early June when penguins are migrating to and/or inhabiting their winter foraging areas. We restricted our isotopic analyses of tail feathers to 18 Adélie (7 male and 11 female) and 34 chinstrap (19 male and 15 female) penguins. These individuals had GLS tracking data that fell within the window of tail-feather synthesis and isotopic incorporation (i.e., 40–100 days following the onset of molt).

The feather sections used for SIA were cleaned using a 2:1 chloroform:methanol rinse, air-dried, and cut into small fragments with stainless steel scissors. We flash-combusted (Costech ECS4010 elemental analyzer) approximately 0.5 mg of each sample loaded into tin cups and analyzed for carbon and nitrogen isotopes ($\delta^{13}\text{C}$ and $\delta^{15}\text{N}$) through interfaced Thermo Scientific Delta V Plus continuous-flow stable isotope ratio mass spectrometer (CFIRMS). Raw δ values were normalized on a two-point scale using glutamic acid reference materials with low and high values (USGS-40: $\delta^{13}\text{C} = -26.4\text{‰}$, $\delta^{15}\text{N} = -4.5\text{‰}$; USGS-41: $\delta^{13}\text{C} = 37.6\text{‰}$, $\delta^{15}\text{N} = 47.6\text{‰}$). Sample precision, based on repeated sampling of

reference materials, was 0.1‰ and 0.2‰ for $\delta^{13}\text{C}$ and $\delta^{15}\text{N}$, respectively. Stable isotope ratios are expressed in δ notation in per mil units (‰), according to the following equation:

$$\delta X = [(R_{\text{sample}}/R_{\text{base}}) - 1] \times 1000$$

where X is ^{13}C or ^{15}N and R_{sample} is the corresponding ratio $^{13}\text{C}/^{12}\text{C}$ or $^{15}\text{N}/^{14}\text{N}$. The R_{base} values were based on the Vienna PeeDee Belemnite (VPDB) for $\delta^{13}\text{C}$ and atmospheric N_2 for $\delta^{15}\text{N}$.

Isotopic niche and dietary modeling

We followed an isotopic niche approach when using SIA to test for inter- and intraspecific foraging niche partitioning (Newsome et al. 2007). When presented as bi-plots, stable isotope values delineate the trophic ($\delta^{15}\text{N}$) and habitat-use ($\delta^{13}\text{C}$) axes of an isotopic niche space (Bodey et al. 2013), which is comparable, although not identical, to the ecological niche space defined by Hutchinson (1959). We used linear models to test for difference in $\delta^{13}\text{C}$ and $\delta^{15}\text{N}$ values between species from the same breeding site as well as within species between breeding sites (chinstrap penguins only). In addition, we tested for differences in species-specific foraging niches between discrete winter foraging areas by classifying chinstrap penguins into two groups (east and west) based on the mean bearing from the tagging location during the period of feather synthesis. We compared the size and degree of overlap in bivariate isotopic niche space ($\delta^{13}\text{C}$ and $\delta^{15}\text{N}$) occupied by chinstrap and Adélie penguins using two methods. First, we calculated the standard ellipse area corrected for sample size (SEA_c ; Jackson et al. 2011). The SEA_c metric is equivalent to a bivariate standard deviation and can be interpreted as a measure of the core isotopic niche of a population (Jackson et al. 2011). We further calculated a Bayesian approximation of SEA_c with corresponding 95% credibility intervals (SEA_b ; Jackson et al. 2011) to quantify uncertainty in core isotopic niche areas. Second, we constructed convex hulls to estimate the smallest total isotopic niche area (TA) that contained all individuals in the isotopic space. The TA metric can be interpreted as a measure of the total isotopic niche of a population (Layman et al. 2007). Using the graphical SEA_c and TA metrics we calculated core and total niche-

overlap indices between groups as both a percentage of overall isotopic area (i.e., niche space) as well as the proportion of individuals of one group encompassed by another group's isotopic area (Hammerschlag-Peyer et al. 2011, Jackson et al. 2011). Isotopic niche modeling was implemented in R (R Core Team 2012).

RESULTS

After one winter of deployment, we recovered 112 tags (69% of deployments) and successfully retrieved location data from 34 Adélie penguins and 57 chinstrap penguins (Table 1). We eliminated 5 Adélie penguins and 5 chinstrap penguins from our analysis due to premature tag failure (prior to the molt) or corrupted location data. The remaining 29 Adélie penguins, all from Admiralty Bay, had a mean active deployment of 211 ± 123 (SD) days. Chinstrap penguins from Admiralty Bay ($N = 19$) had a mean active deployment of 141 ± 78 (SD) and chinstraps from Cape Shirreff ($N = 33$) had a mean active deployment of 121 ± 67 (SD) days.

Habitat utilization

During winter, chinstrap penguins generally exhibited a higher diversity of individual movement patterns, undertook longer-distance movements, and occupied a broader geographic range of marine habitats than Adélie penguins. Chinstrap penguins exhibited two main movement modes, migrating either west or east from tagging locations in the South Shetland Islands (Figs. 2A, 3). The majority of chinstraps from Cape Shirreff (82%) and Admiralty Bay (63%) migrated west into the Pacific sector of the Southern Ocean while the remainder moved east into the south Atlantic sector. Individual chinstrap penguins migrated as far west as 138° W and as far east as 30° W prior to instrument failure, representing maximum point-to-point great-circle distances from tagging locations of 3900 km and 1960 km, respectively. These maximum distances were achieved within 3 months of the end of the molting period and prior to late June/early July when the data suggest that the birds reversed course and initiated their return migrations (Figs. 2A, 3). The latitudes used by chinstraps throughout the winter, whether moving east or west from the

South Shetland Islands, remained in a relatively narrow band between 60° S and 65° S (Fig. 2B), generally bounded on the south by advancing sea ice edge and to the north by the 2° C isotherm (Fig. 3). Average daily sea surface temperatures recorded by the GLS tags ($1.3^\circ\text{C} \pm 2.8^\circ\text{C}$ mean \pm SD) and the spatial distribution of those temperatures (Appendix C) corroborate this broad-scale characterization of winter habitat.

In contrast, all Adélie penguins tagged in this study exhibited a counter-clockwise movement pattern (Figs. 2C, D, 3). After the breeding season, all tagged individuals moved southeast into the NW Weddell Sea where, presumably, all individuals molted (e.g., Dunn et al. 2011). Incomplete data for the month of March, due to location errors associated with the equinox (Ekstrom 2004), precluded clear interpretation of movements immediately following the molt, but by mid-April most individuals had returned as far north at 60° S (Fig. 2D). Thereafter, movement was relatively restricted and all individuals appeared to remain in the southern Scotia Sea and northwestern Weddell Sea between 50° W and 60° W longitude, without appreciable directional movement until return trips to the breeding colonies commenced by late September. The mean great circle distance to the tagging location in Admiralty Bay during the mid-winter period (June–August) for all Adélie penguins combined was 555 ± 248 km. The tracking data suggest that Adélie penguins occupied habitats centered on ice concentrations between 15 and 50% for most of the winter (Fig. 3). Average daily sea surface temperatures recorded by the GLS tags ($-1.2 \pm 4.9^\circ\text{C}$; Appendix C), further suggest the occupation of habitats with sea ice cover.

The level of spatial overlap differed between and within species. Due to the large-scale longitudinal movements of most chinstrap penguins in ice-free waters, the index of spatial overlap of winter habitats used by chinstrap and Adélie penguins was relatively low and generally decreased as winter progressed (Fig. 4A). In general, the probability of co-occurrence of Adélie and chinstrap penguins in a given grid cell was low (<0.004) throughout the winter (Fig. 5), but areas of co-occurrence were consistently located in the confluence of the Weddell and Scotia Seas between Elephant Island and the

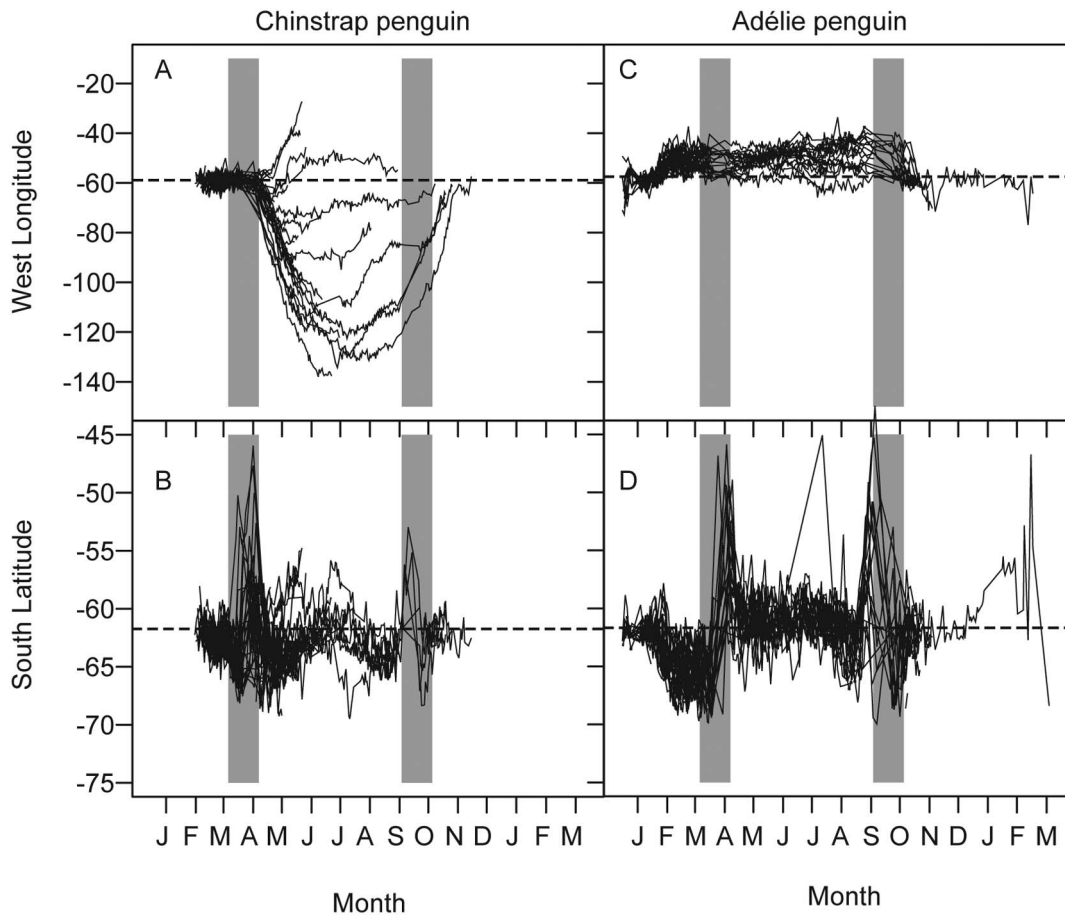


Fig. 2. Bias-corrected latitude and longitude tracks from all chinstrap and Adélie penguins recovered with geolocation loggers. Gray bars indicate a three week period centered on the vernal and autumnal equinoxes when location estimates from GLS instruments are inaccurate. Dashed lines indicating mean latitude and longitude of tag release sites in the South Shetland Islands, respectively, are included for reference.

South Orkney Islands. The periods with highest overlap occurred in March and November, months that are immediately adjacent to the main summer breeding season. Relatively high overlap in March can be attributed to the northward movement into the Scotia Sea of Adélie penguins after their molt and the initial eastward migration of some chinstraps away from breeding colonies following the breeding season. Similarly, the relatively high overlap in November can be attributed to return migrations of both species and occupancy of habitats near their original tagging locations prior to the start of the breeding season.

An index of individual overlap, based on the proportion of the tagged population that occu-

pled a particular grid cell, was correlated with the spatial overlap index (Pearson's product moment: $r = 0.75$, $t_8 = 3.2$, $P = 0.01$) and further suggested that the periods with higher spatial overlap were driven by numerous individuals that exhibited occupancy in the same grid cells. Therefore, while the spatial extent of overlap was small, some areas were visited by many individuals from both species.

Spatial and individual overlap among chinstraps was generally higher than the overlap observed between chinstrap and Adélie penguins. Intra-specific spatial overlap of chinstrap penguins from Cape Shirreff and Admiralty Bay exceeded 50% during the early winter period and was generally higher than inter-specific overlap

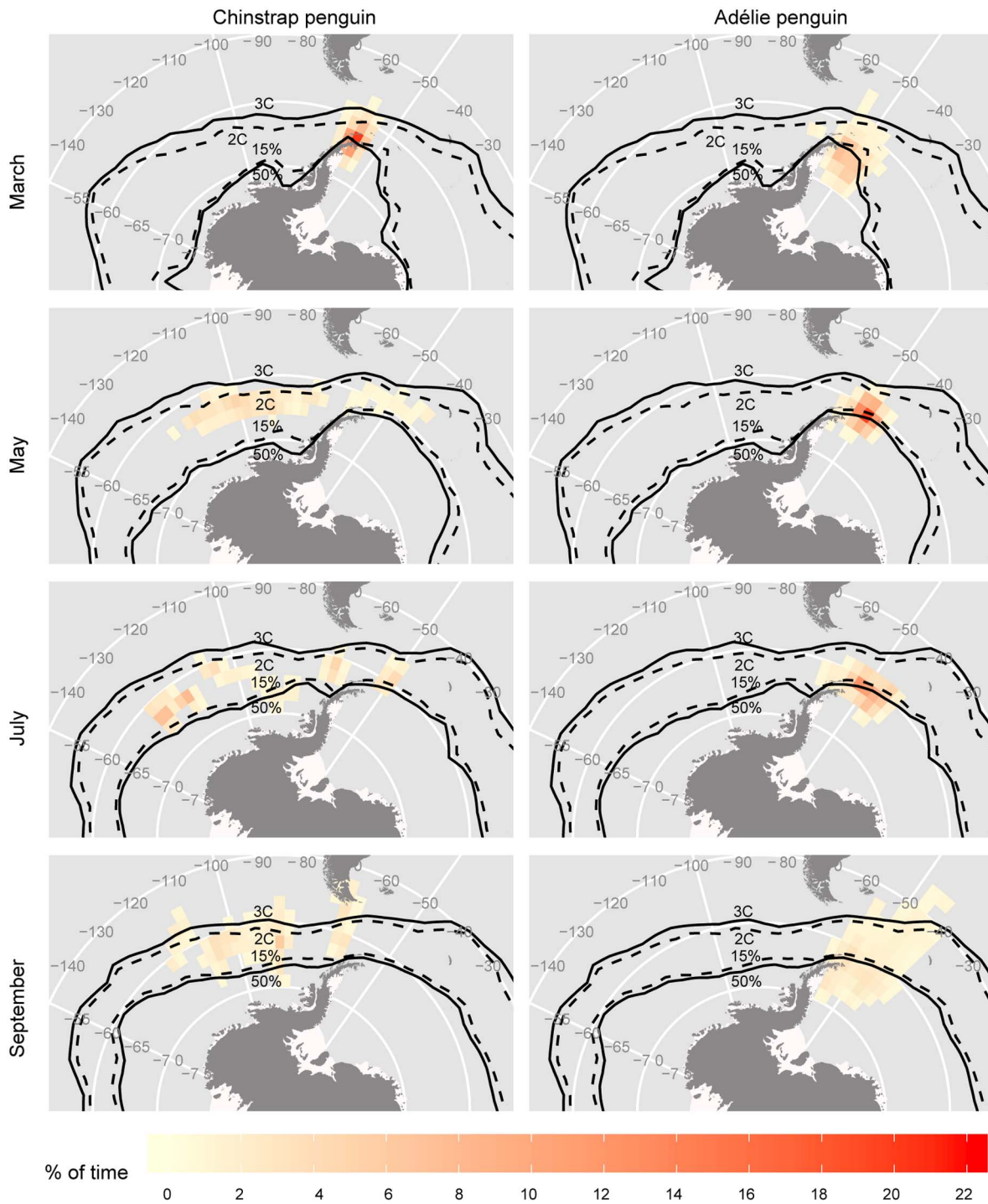


Fig. 3. Representative habitat utilization during winter months for chinstrap and Adélie penguins in March, May, July, and September. Isotherms for 2°C and 3°C and contours for 15% and 50% sea ice concentration are plotted for reference. Maps for all winter months for each species are included in Appendix C.

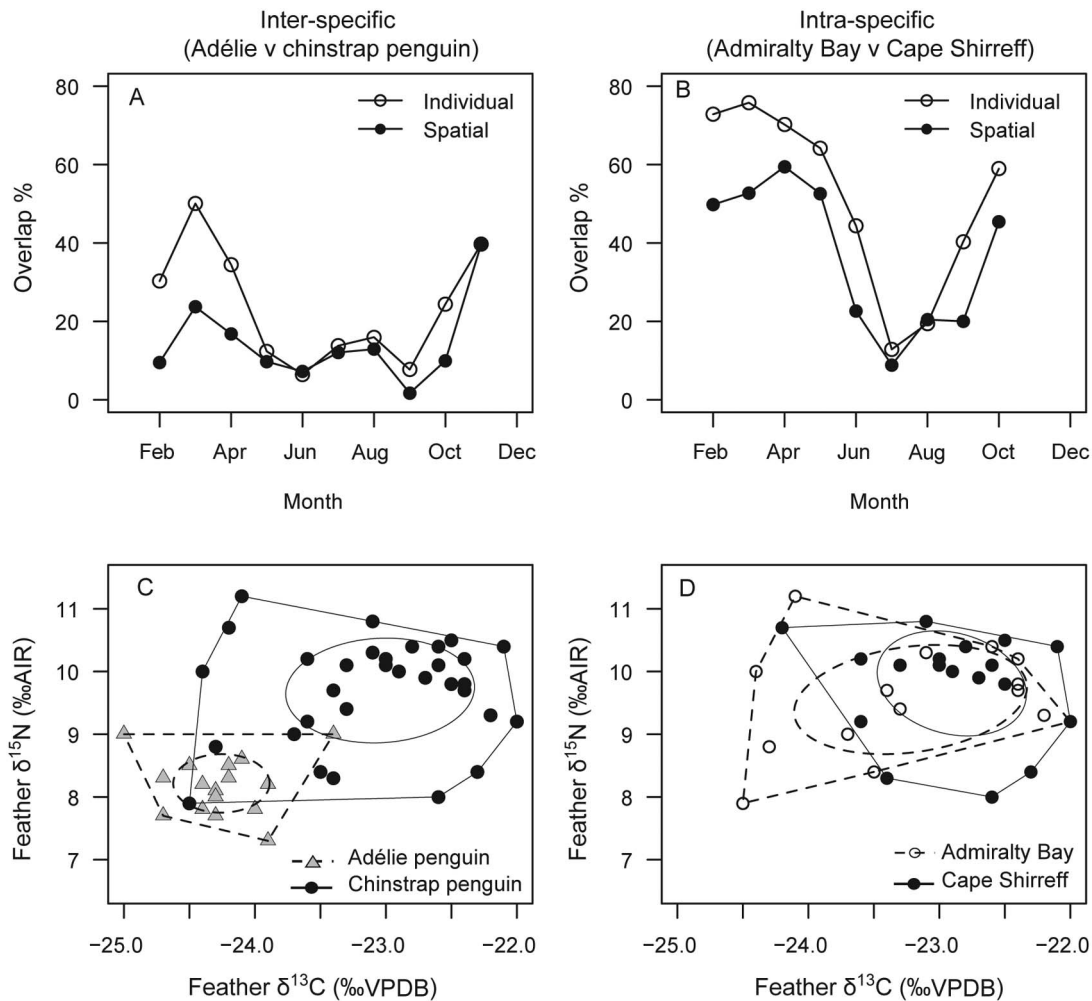


Fig. 4. Indices of spatial overlap and stable isotopic signatures for (A) Spatial and individual indices of overlap between Adélie and all chinstrap penguins. (B) Index of spatial overlap among chinstrap penguins from Admiralty Bay and Cape Shirreff. (C) Stable isotope values with estimates of core (SEA_c ; ellipses) and total niche areas (TA; convex polygons) for Adélie and all chinstrap penguins. (D) Stable isotope values with estimates of core (SEA_c ; ellipses) and total niche areas (TA; convex polygons) for chinstrap penguins from Admiralty Bay and Cape Shirreff.

throughout the winter (Fig. 4B). The relatively high overlap during the early winter period again suggested common migratory corridors for chinstraps with minimal segregation of spatial habitats based on natal colony. As winter progressed a decline in overlap was observed (Fig. 4B) that could be attributed to spatial segregation as individuals chose foraging grounds scattered across the wide range of longitudes (Fig. 3).

Isotopic niche

Stable isotope values of tail feathers and the extent of overlap in niche space differed between and within species. Both $\delta^{13}C$ ($F_{1,50} = 46.01$, $P < 0.01$) and $\delta^{15}N$ ($F_{1,50} = 49.95$, $P < 0.01$) differed between species, with mean carbon and nitrogen isotope values higher in chinstrap relative to Adélie penguins (Table 2, Fig. 4C). Core and total isotopic niche sizes were also larger in chinstrap penguins compared to Adélie penguins (Table 2). Generally, core isotopic niches overlapped little

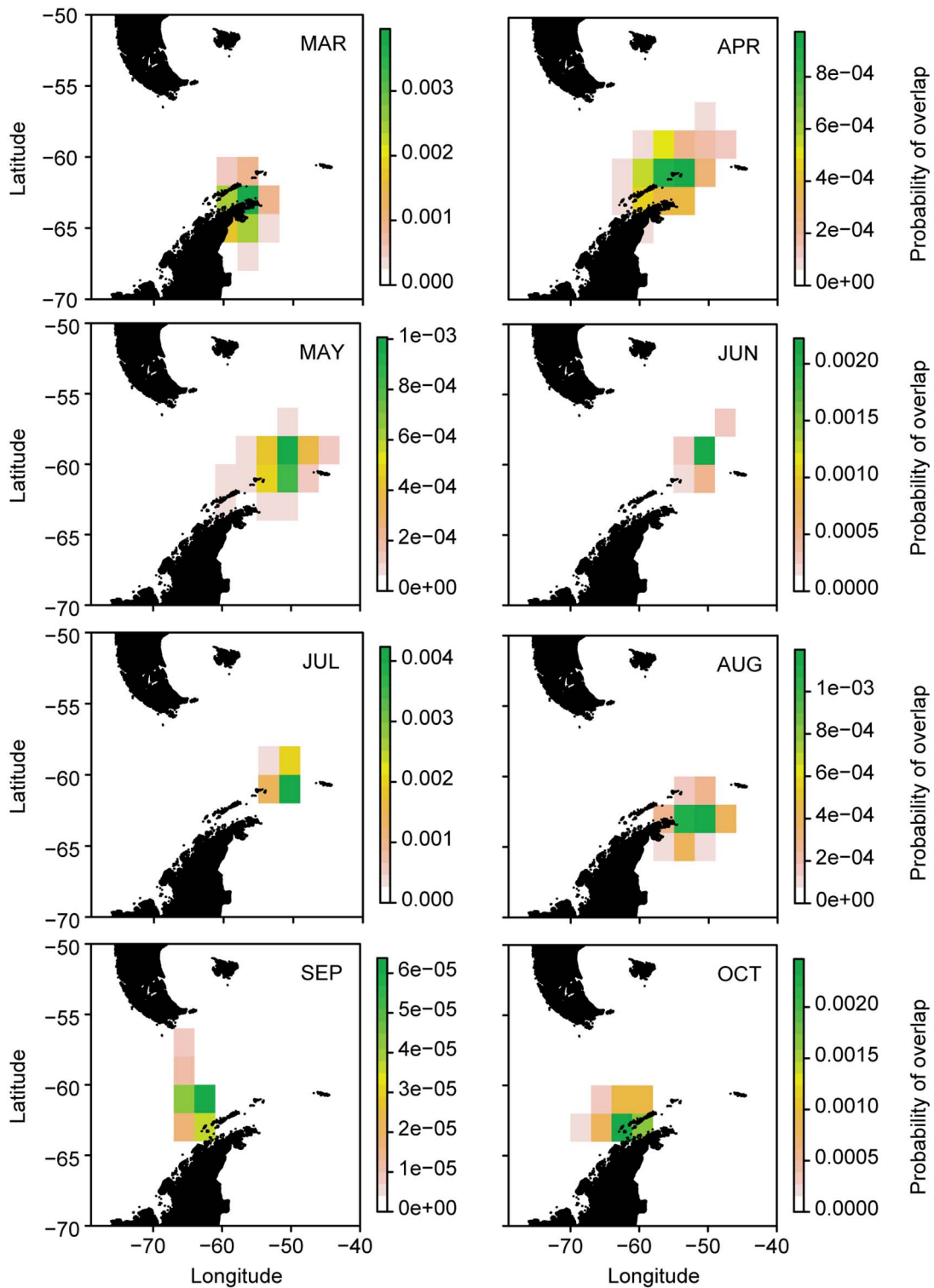


Fig. 5. Maps of monthly joint probability of spatial overlap for Adélie and chinstrap penguins.

Table 2. Tail feather stable carbon ($\delta^{13}\text{C}$) and nitrogen ($\delta^{15}\text{N}$) isotopic values, core (SEA_b) and total (TA) isotopic niche area during the early winter period (40–100 days post molt) in Adélie and chinstrap penguins instrumented with GLS devices from the South Shetland Islands. Chinstrap penguins are further divide by breeding site (AB: Admiralty Bay; CS: Cape Shirreff) and those undergoing eastwards (east) and westward (west) migrations from the South Shetland Islands. Values in parentheses represent 95% credibility intervals.

Species	<i>N</i>	$\delta^{13}\text{C}$ (‰)	$\delta^{15}\text{N}$ (‰)	SEA_b (‰)	TA (‰)
Adélie	18	-24.3 ± 0.3	8.2 ± 0.4	0.9 (0.6–1.3)	1.9
Chinstrap (all)	34	-23.0 ± 0.7	9.7 ± 0.8	2.0 (1.5–2.6)	6.5
Chinstrap (AB)	15	-23.2 ± 0.8	9.6 ± 0.8	2.4 (1.6–3.8)	4.8
Chinstrap (CS)	19	-22.9 ± 0.6	9.8 ± 0.8	1.5 (1.2–2.5)	4.2
Chinstrap (west)	28	-22.8 ± 0.6	9.9 ± 0.7	1.4 (1.0–1.9)	4.0
Chinstrap (east)	6	-24.0 ± 0.5	8.7 ± 0.7	2.2 (1.1–4.0)	1.2

between Adélie and chinstrap penguins (0.0% of core niche area and 2.9–5.6% of individuals with the core area; Fig. 4C), though there was a larger and more variable degree of overlap when examining total niche space (15.3–54.2% of total area and 8.8–44.4% of individuals within the total area; Fig. 4C). Within a species, however, chinstrap penguins from different breeding sites exhibited no difference in mean tail-feather $\delta^{13}\text{C}$ ($F_{1,32} = 1.68$, $P = 0.20$) and $\delta^{15}\text{N}$ ($F_{1,32} = 0.81$, $P = 0.37$; Table 2, Fig. 4D). The niche areas of chinstrap penguins from Admiralty Bay and Cape Shirreff exhibited a higher degree of overlap in core niche space (54.2–87.7% of core area and 40.0–47.4% of individuals within the core area) and total niche space (64.7–73.8% of total area and 60.0–68.4% of individuals with the total area) between sites (Fig. 4D).

When GLS tracked penguins were divided by species and eastward vs. westward migration patterns (Fig. 6A), we found differences in spatial overlap, isotopic values, and isotopic niche space. Spatial overlap during the period of feather growth was highest for Adélie penguins and those chinstrap penguins that exhibited eastward migrations (Fig. 6B). The Adélie and eastward migrating chinstrap penguins had similar $\delta^{13}\text{C}$ ($F_{1,22} = 4.29$, $P = 0.05$) and $\delta^{15}\text{N}$ ($F_{1,22} = 2.46$, $P = 0.13$) values in their tail feathers while chinstraps that exhibited westward migration patterns had different $\delta^{13}\text{C}$ ($F_{1,50} = 89.23$, $P > 0.01$) and $\delta^{15}\text{N}$ ($F_{1,50} = 77.43$, $P > 0.01$) tail-feather values relative to all eastward moving birds (Fig. 6C). Correspondingly, Adélie and eastward migrating chinstrap penguins had a high degree of overlap in core niche space (19.0–49.4% of core area and 16.7–22.2% of individuals within the core area) and total niche space (45.0–68.2% of total area

and 38.9–50.0% of individuals within the total area; Fig. 6C). Chinstrap penguins that exhibited a westward migration pattern had lower isotopic overlap (0.0% of core niche space and 0.0–3.6% of individuals) with eastward migrating penguins (Fig. 6C).

DISCUSSION

In this study we simultaneously tracked Adélie and chinstrap penguins from adjacent breeding colonies during the austral winter. The area of marine habitat used by chinstrap and Adélie penguins tagged from the South Shetland Islands was expansive, covering over 100° of longitude, and occupying a variable latitudinal range bounded by advancing pack ice in the south and the 2°C isotherm in the north. Such large-scale occupancy of marine habitats from two small seabird colonies in the South Shetland Islands highlights the mobility of these penguin species and the general suitability of vast expanses of the Southern Ocean pelagic region as winter habitat for chinstrap and Adélie penguins. The majority of observations indicate that inter-specific overlap of habitat during the non-breeding season is minimal, while intra-specific overlap by chinstraps from adjacent breeding colonies was higher. These results indicate spatial segregation is the primary mechanism of inter-specific niche separation during winter for Adélie and chinstrap penguins. However, it is important to note that a pelagic corridor along the confluence of the Weddell and Scotia Seas was occupied by chinstrap and Adélie penguins for most months of the year. Moreover, the eastward-migrating chinstrap and Adélie penguins had similar stable isotope signatures

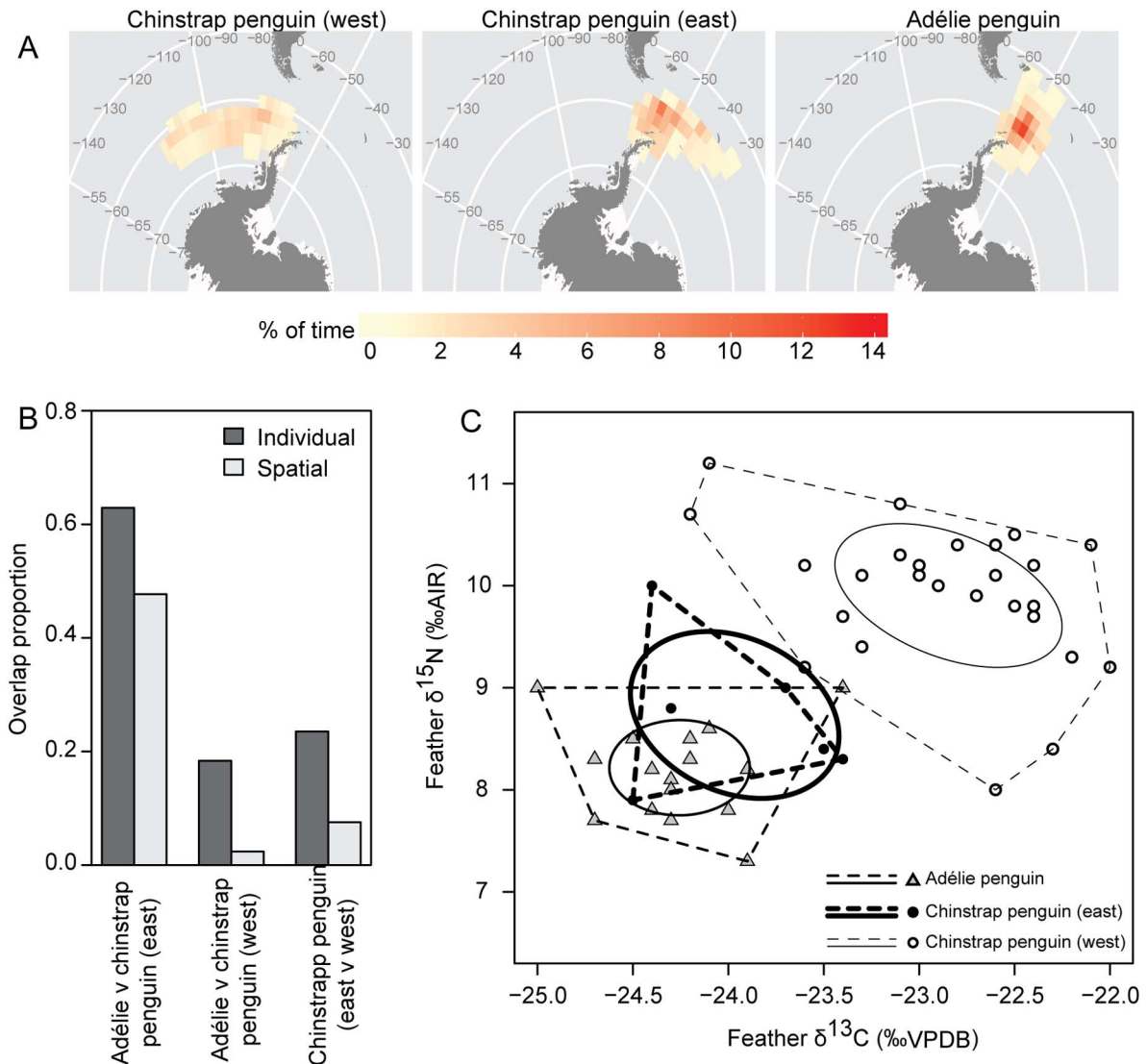


Fig. 6. Indices of (A) habitat utilization, (B) spatial and individual overlap, and (C) stable isotopic signatures of tail feathers from chinstrap and Adélie penguins exhibiting eastern or western migration patterns during the period of tail feather synthesis. Core isotopic niche space (SEA_c; solid ellipses) and total isotopic niche space (TA; dashed convex hulls) for each grouping are identified.

during the final period of tail-feather growth, suggestive of shared isotopic niche space during this early winter period. There is, therefore, the potential for inter-specific competition during winter for this species pair.

Consistent with shipboard observations (Ainley et al. 1994), we found relatively strong evidence for species-specific segregation during winter with the 15% ice-concentration contour providing a general boundary to separate suit-

able habitats for Adélie and chinstrap penguins for the duration of the non-breeding season. Nonetheless, an important area along the confluence of the Scotia and Weddell Seas was identified where overlap exceeded 47% for spatial and individual metrics of occupancy by Adélie and the eastward migrating chinstrap penguins during the isotope measurement period (April and May). Isotopic niches also suggested overlap in this area during the early

winter migration period. The spatial and isotopic overlap observed during the early winter migration period suggests the importance of this marine habitat for both species. For example, post-molt mass of adult chinstrap penguins is typically 81% of typical mass during the breeding season (US AMLR, *unpublished data*). Feeding conditions and the potential for competition for shared resources immediately following the molt may therefore be critical for recovery of body mass and, ultimately, survival.

Mechanisms that reinforce intra-specific spatial niche separation among Adélie penguins may include colony-specific patterns in dispersal from breeding colonies that help minimize overlap with other breeding populations. We have tracked individuals from one small colony, but it is useful to compare their dispersal patterns with those from other studies. For example, data from Adélie penguins tracked from Marguerite Bay, along the southwestern Antarctic Peninsula, demonstrate relatively local movements constrained by the development and advection of sea ice from the Bellingshausen Sea northward along the western Antarctic Peninsula (Erdmann et al. 2011); birds from the South Orkney Islands exhibited larger-scale southward movements into the Weddell Sea (Dunn et al. 2011); and Adélie penguins from colonies in the Ross Sea and along East Antarctica must migrate north to the marginal ice zone and daylight during winter (Clarke et al. 2003, Ballard et al. 2010). Among Adélie penguins, movement patterns appear to be dictated by the location of a breeding colony relative to the advancing winter sea ice. Adélie penguins from Admiralty Bay conform to this general model by first moving south into ice-covered areas in the Weddell Sea and then moving north as the ice edge advanced. Such migratory dependencies based on colony location relative to the nearest sea ice edge may help maintain colony or meta-population (Ainley et al. 1995) segregation at sea for Adélie penguins.

Winter tracking studies of chinstrap penguins are comparatively scarce, but two studies from the South Shetland Islands suggested a mixture of movement patterns that include retention near breeding colonies during early winter versus larger-scale (>1000 km), directed eastward movement toward the South Orkney and South Sandwich Islands along the confluence of the

Scotia and Weddell seas (Wilson et al. 1998, Trivelpiece et al. 2007). We observed these patterns and add a third major pattern of large-scale westward movement into remote pelagic regions of the Bellingshausen and Amundsen Seas. The westward migration was the most commonly observed movement pattern of chinstrap penguins from Cape Shirreff (81% of deployments) and Admiralty Bay (63% of deployments). The large-scale westward movement challenges the hypothesis forwarded by Trivelpiece et al. (2007) that proposed the main migratory directions exhibited by individuals was related to the location of ancestral source populations. The high degree of westward movement is therefore curious because there are no major chinstrap colonies west of the South Shetland Islands that could be a potential source population. It is unknown if this westward movement pattern has developed since earlier tracking studies were conducted or whether previous tracking studies from the South Shetland Islands did not reveal this behavior because sample sizes were small (Wilson et al. 1998, Trivelpiece et al. 2007). Of note, Ratcliffe et al. (2014) reported that the macaroni (*Eudyptes chrysolophus*) and rockhopper (*E. chrysocome*) penguins tracked from South Georgia and the Falkland Islands exhibited high rates of occupancy in the Scotia Sea during winter. The westward movement of chinstrap penguins from the Peninsula region may, therefore, be a behavioral response to avoid high densities of these *Eudyptes* penguins in the central Scotia Sea. Regardless, it is clear that suitable winter foraging areas for chinstrap penguins from the Antarctic Peninsula region span a wide longitudinal range that includes the ice-free Pacific sector of the Southern Ocean.

Despite the widespread use of large swaths of the Southern Ocean, we do not find strong evidence for colony-specific spatial segregation during winter. All chinstraps moved along similar eastern or western corridors at similar times and exhibited broad overlap in ice free pelagic areas throughout the winter. The reduced spatial overlap of chinstraps from different colonies that was estimated for mid-winter months can be partially attributed to selection of different termination points for each individual, rather than a colony-specific preference for

separate areas. For example, the tracking data demonstrate that individual differences existed in the rate of westward movement, selection of over-winter foraging grounds, and commencement of return migration (Fig. 2). Such individual-based selection results in a more diffuse distribution across wide swaths of suitable chinstrap habitat in the Southern Ocean that tends to reduce estimates of overlap. Alternatively, we note that diminishing sample sizes as the number of tag failures increased could also account for the reduced overlap in mid-winter. Nonetheless, the observation of generally high winter overlap of birds from different breeding colonies supports our original hypothesis that overlap of chinstraps would occur, and provides a contrast with recent studies on *Eudyptes* penguins. Thiebot et al. (2011) reported fully distinct winter habitats for macaroni penguins (*E. chrysolophus*) tracked from Crozet and Kerguelen Islands, colonies separated by 1400 km. Similarly, Ratcliffe et al. (2014) demonstrated distinct winter foraging areas among southern rockhopper penguins (*E. chrysocome chrysocome*) from colonies separated by 250 km on the Falkland Islands.

The above species-specific differences in spatial overlap during the non-breeding season may depend on the size and proximity of the two breeding populations considered. Ainley et al. (1995) hypothesized that adjacent colonies may act more as a meta-population rather than a set of strictly independent breeding aggregations. We note that the two tagging locations for chinstrap penguins in this study were much closer (120 km) than either of the other studies (>250 km). While foraging ranges of conspecifics from adjacent colonies seldom overlap during the breeding season (Wilson 2010), presumably due to predictable aggregations of high-density prey near colony locations (Fraser and Trivelpiece 1996), the relatively high degree of overlap of chinstraps from our study sites during winter corroborates this meta-population hypothesis. Specifically, the overlap facilitates contact and potential mixing of individuals from multiple breeding locales. We further suggest that the small and regionally declining breeding clusters of chinstrap penguins in the Antarctic Peninsula region may be responding to large-scale drivers (Trivelpiece et al. 2011). The observation of

shared occupancy of wide swaths of the Southern Ocean during winter suggests a mechanism, namely shared winter habitats, by which a meta-population could exhibit similar long-term trends across distinct breeding locations.

We identified a differentiation of isotopic niche space from late-grown sections of tail feathers that was correlated with the movement patterns of our study birds. This suggests that large-scale migration patterns in Adélie and chinstrap penguins may be estimable from SIA of tail feathers. However, linking animal movement patterns with variation in tissue stable isotope values relies on an understanding of the timing of tissue synthesis and any possible lags between resource acquisition and mobilization for tissue growth (Bearhop et al. 2002, Martínez del Rio et al. 2009, Ramos and González-Solís 2012). Nonetheless, there are several lines of evidence to support our inference.

First, the captive growth study demonstrated that tail feather growth is completed after the main body plumage molt (Appendix B). Second, while there is relatively less empirical data available on the isotopic turn-over of feathers, turn-over rates of whole blood and feathers appear to be similar (Bearhop et al. 2002). Studies of captive African penguins (*Spheniscus demersus*) indicate that whole blood integrates dietary information over a period 20 days (Barquete et al. 2013), though turn-over rates are predicted to be faster in wild birds due to higher metabolic rates (Bearhop et al. 2002). Using this conservative 20-day window as a benchmark and the likely timing of synthesis for tail feather section used in our analysis (59 ± 11 and 69 ± 20 days after the on-set of molt for chinstrap and Adélie penguins, respectively), the earliest isotopic signal observed in our data may therefore reflect a time period averaged from 38–59 days and 49–69 days after the onset of molt, respectively. At these times, the molt fast was over, migrations to winter foraging habitat were underway, and geographic separation existed between birds moving mainly east or west. Finally, we note that penguins are in the poorest body condition of their annual cycle following the fast that accompanies the body-plumage molt (Adams and Brown 1990). Once the body molt is complete, the birds commence migrations to wintering habitats, and resume feeding to recov-

er critical body reserves while at the same time completing tail feather growth. While we must make assumptions about mobilization of any remaining body reserves versus routing of new consumption to tail feather growth, several observations suggest that resource consumption during migration fuels tail feather synthesis. First, the diets of adult chinstrap and Adélie penguins at the study colonies during the summer breeding season are similar across individuals, consistent over the course of the breeding season, and similar year after year (Hinke et al. 2007). Second, isotope values from feathers grown in fledgling chicks (reflecting summer diets provided by the adult) also exhibit very low inter-individual variation (Cherel and Hobson 2007, Polito et al. 2015). This leads to an expectation that tail feather isotope values of all individuals, particularly within a species from the same breeding locations, would be similar if feather synthesis was dependent on pre-molt (summer) diets or body reserves. In contrast, we observed different isotopic values from birds with contrasting movement patterns, suggesting that resource consumption during migration fuels tail feather synthesis.

Although our sample sizes are relatively small, the degree of differentiation observed in the isotopic niche space among individuals migrating into Pacific or Atlantic sectors of the Southern Ocean suggests that basin-scale differences in the isotopic composition of penguin prey resources are reflected in their tissues. The observed differences within and between species indicate that isotope signatures from penguin tail feathers may be a useful tracer for identifying large-scale movement patterns of Adélie and chinstrap penguins, similar to other Southern Ocean seabirds (e.g., Cherel and Hobson 2007, Phillips et al. 2009, Jaeger et al. 2010, Quillfeldt et al. 2010). However, it is important to note that consumer stable isotope values can change over time due to shifts in dietary composition or movement between geographic location with differing isotopic baselines (e.g., Cherel and Hobson 2007, Brasso and Polito 2013, McMahon et al. 2013). These factors make it difficult to determine if the difference in isotopic niche space observed between individuals migrating into Pacific or Atlantic sectors of the Southern Ocean may arise from different diets, variation in

baseline stable isotopes values, or some combination of the two. Studies using techniques that can differentiate between these two factors, such as the compound specific-stable isotope analysis of amino acids, are advisable in the future (McMahon et al. 2013).

Conclusions

A goal of miniaturization of tagging technologies and isotopic study of body tissues, particularly for migrating animals in marine environments, is to allow the identification of foraging locations without the need for expensive and invasive sampling techniques. By integrating light-based geolocation data and estimates of isotopic niche from the analysis of ^{13}C and ^{15}N composition of tail feathers, we revealed widespread use of the Southern Ocean by chinstrap penguins. The results suggest relatively broad intra-specific overlap of winter habitats for chinstrap penguins from two breeding colonies in the South Shetland Islands, in contrast with the large-scale spatial segregation of winter foraging habitats used by Adélie and chinstrap penguins. However, the confluence of the Weddell and Scotia Seas was an area in which both species exhibited consistent spatial and isotopic overlap. This confluence region represents a critical corridor for early winter movements and feeding conditions there may impact recovery of post-molt body mass and survival. Finally, the separation of isotopic niche space that was correlated with the large-scale movement patterns suggests the ability to estimate basin-scale movements of penguins on a population level via large-scale collection of feathers. Such population-level estimates of habitat use, while necessarily coarse in resolution, may provide novel monitoring opportunities for these highly mobile seabirds in the future.

ACKNOWLEDGMENTS

We thank M. Mudge, N. Cook, M. Goh, S. Triveliece, P. Chilton, B. Soucie, M. Henschen, C. Bishop, and A. Bertoldi for assistance deploying and recovering tags for this study. Funds for the GLS tags were provided by the National Marine Sanctuary Foundation. Thank you also to S. Branch and the aviculture department at SeaWorld Orlando for assistance in measuring penguin tail feather growth rates. Additional support for this project was provided by a

Woods Hole Oceanographic Devonshire Scholarship as well as funding from the Ocean Life Institute and SeaWorld Bush Gardens Conservation Fund to MJJ. Reference to any specific commercial products, process, or service by trade name, trademark, manufacturer, or otherwise, does not constitute or imply its recommendation, or favoring by the United States Government or NOAA/National Marine Fisheries Service. Use of information from this publication shall not be used for advertising or product endorsement purposes. The Antarctic fur seal portion of this study (mobile control tags) was conducted under the Marine Mammal Protection Act Permit #16472-01. All protocols were reviewed and approved by the UCSD IACUC.

LITERATURE CITED

- Adams, N. J., and C. R. Brown. 1990. Energetics of molt. Pages 297–315 in L. S. Davis and J. T. Darby, editors. *Penguin biology*. Academic Press, San Diego, California, USA.
- Ainley, D. G., N. Nur, and E. J. Woehler. 1995. Factors affecting the distribution and size of Pygoscelid penguin colonies in the Antarctic. *Auk* 112:171–182.
- Ainley, D. G., C. A. Ribic, and W. R. Fraser. 1994. Ecological structure among migrant and resident seabirds of the Scotia-Weddell confluence region. *Journal of Animal Ecology* 63:347–364.
- Ballard, G., V. Toniolo, D. G. Ainley, C. L. Parkinson, K. R. Arrigo, and P. N. Trathan. 2010. Responding to climate change: Adélie penguins confront astronomical and ocean boundaries. *Ecology* 91:2056–2069.
- Barquete, V., V. Strauss, and P. G. Ryan. 2013. Stable isotope turnover in blood and claws: a case study in captive African Penguins. *Journal of Experimental Marine Biology and Ecology* 448:121–127.
- Bearhop, S., S. Waldron, S. C. Votier, and R. W. Furness. 2002. Factors that influence assimilation rates and fractionation of nitrogen and carbon stable isotopes in avian blood and feathers. *Physiological and Biochemical Zoology* 75:451–458.
- Biuw, M., C. Lydersen, P. J. Nico de Bruyn, A. Arriola, G. G. J. Hofmeyr, P. Kritzing, and K. M. Kovacs. 2010. Long-range migration of a chinstrap penguin from Bouvetøya to Montagu Island, South Sandwich Islands. *Antarctic Science* 22:157–162.
- Block, B. A., et al. 2011. Tracking apex marine predator movements in a dynamic ocean. *Nature* 475:86–90.
- Bodey, T. W., E. J. Ward, R. A. Phillips, R. A. McGill, and S. Bearhop. 2013. Species versus guild level differentiation revealed across the annual cycle by isotopic niche examination. *Journal of Animal Ecology* 83:470–478.
- Bond, A. L., and L. L. Jones. 2009. A practical introduction to stable-isotope analysis for seabird biologists: approaches, cautions and caveats. *Marine Ornithology* 37:183–188.
- Bost, C. A., J. B. Charrassin, Y. Clerquin, Y. Ropert-Coudert, and Y. Le Maho. 2004. Exploitation of distant marginal ice zones by king penguins during winter. *Marine Ecology Progress Series* 283:293–297.
- Brasso, R. L., and M. J. Polito. 2013. Trophic calculations reveal the mechanism of population-level variation in mercury concentrations between marine ecosystems: case studies of two polar seabirds. *Marine Pollution Bulletin* 75:244–249.
- Cherel, Y., and K. A. Hobson. 2007. Geographical variation in carbon stable isotope signatures of marine predators: a tool to investigate their foraging areas in the Southern Ocean. *Marine Ecology Progress Series* 329:281–287.
- Cherel, Y., M. Le Corre, S. Jaquemet, F. Menard, P. Richard, and H. Weimerskirch. 2008. Resource partitioning within a tropical seabird community: new information from stable isotopes. *Marine Ecology Progress Series* 366:281–291.
- Clarke, J., K. Kerry, C. Fowler, R. Lawless, S. Eberhard, and R. Murphy. 2003. Post-fledging and winter migration of Adélie penguins *Pygoscelis adeliae* in the Mawson region of East Antarctica. *Marine Ecology Progress Series* 248:267–278.
- Connan, M., C. D. McQuaid, B. T. Bonnevie, M. J. Smale, and Y. Cherel. 2014. Combined stomach content, lipid and stable isotope analyses reveal spatial and trophic partitioning among three sympatric albatrosses from the Southern Ocean. *Marine Ecology Progress Series* 497:259–272.
- Croxall, J. P., P. A. Prince, and K. Reid. 1997. Dietary segregation of krill-eating South Georgia seabirds. *Journal of Zoology* 242:531–556.
- Dunn, M. J., J. R. D. Silk, and P. N. Trathan. 2011. Post-breeding dispersal of Adélie penguins (*Pygoscelis adeliae*) nesting at Signy Island, South Orkney Islands. *Polar Biology* 34:205–214.
- Ekstrom, P. A. 2004. An advance in geolocation by light. *Memoirs of the National Institute of Polar Research, Special Issue* 58:210–226.
- Erdmann, E. S., C. A. Ribic, D. L. Patterson-Fraser, and W. R. Fraser. 2011. Characterization of winter foraging locations of Adélie penguins along the Western Antarctic Peninsula, 2001–2002. *Deep Sea Research II* 58:1710–1718.
- Fraser, W. R., and W. Z. Trivelpiece. 1996. Factors controlling the distribution of seabirds: winter-summer heterogeneity in the distribution of Adélie penguin populations. Pages 257–272 in R. M. Ross, E. E. Hofmann, and L. B. Quetin, editors. *Foundations for ecological research west of the Antarctic Peninsula*. American Geophysical Union, Washing-

- ton, D.C., USA.
- Freitas, C., C. Lydersen, R. A. Ims, M. A. Fedak, and K. M. Kovacs. 2008. A simple new algorithm to filter marine mammal Argos locations. *Marine Mammal Science* 24:315–325.
- González-Solís, J., J. P. Croxall, D. Oro, and X. Ruiz. 2007. Trans-equatorial migration and mixing in the wintering areas of a pelagic seabird. *Frontiers in Ecology and the Environment* 5:297–301.
- Hammerschlag-Peyer, C. M., L. A. Yeager, S. M. Araújo, and C. A. Layman. 2011. A hypothesis-testing framework for studies investigating ontogenetic niche shifts using stable isotope ratios. *PLoS ONE* 6:e27104.
- Hinke, J. T., K. Salwicka, S. G. Trivelpiece, G. M. Watters, and W. Z. Trivelpiece. 2007. Divergent responses of *Pygoscelis* penguins reveal a common environmental driver. *Oecologia* 153:845–855.
- Hinke, J. T., S. G. Trivelpiece, and W. Z. Trivelpiece. 2014. Adélie penguin (*Pygoscelis adeliae*) survival rates and their relationship to environmental indices in the South Shetland Islands, Antarctica. *Polar Biology* 37:1797–1809.
- Hobson, K. A. 1999. Tracing origins and migration of wildlife using stable isotopes: a review. *Oecologia* 120:314–326.
- Hutchinson, G. E. 1959. Homage to Santa Rosalia, or why are there so many kinds of animals? *American Naturalist* 93:145–159.
- Inger, R., and S. Bearhop. 2008. Applications of stable isotope analyses to avian ecology. *Ibis* 150:447–461.
- Jackson, A. L., R. Inger, C. A. Parnell, and S. Bearhop. 2011. Comparing isotopic niche widths among and within communities: SIBER—Stable Isotope Bayesian Ellipses in R. *Journal of Animal Ecology* 80:595–602.
- Jaeger, A., V. J. Lecomte, H. Weimerskirch, P. Richard, and Y. Cherel. 2010. Seabird satellite tracking validates the use of latitudinal isoscapes to depict predators' foraging areas in the Southern Ocean. *Rapid Communications in Mass Spectrometry* 24:3456–3460.
- Johnson, D., J. London, M.-A. Lea, and J. Durban. 2008. Continuous-time correlated random walk model for animal telemetry data. *Ecology* 89:1208–1215.
- Karnovsky, N., D. G. Ainley, and P. Lee. 2007. The impact and importance of production in polynyas to top trophic predators: three case studies. Pages 391–410 in W. O. Smith, Jr. and D. G. Barber, editors. *Polynyas: windows to the world*. Elsevier, Amsterdam, The Netherlands.
- Kooyman, G. L., E. C. Hunke, S. F. Ackley, R. P. van Dam, and G. Robertson. 2000. Moulting of the emperor penguin: travel, location, and habitat selection. *Marine Ecology Progress Series* 204:269–277.
- Layman, C. A., D. A. Arrington, C. G. Montaña, and D. M. Post. 2007. Can stable isotope ratios provide for community-wide measures of trophic structure? *Ecology* 88:42–48.
- Lewis, S., T. N. Sherratt, K. C. Hamer, and S. Wanless. 2001. Evidence of intra-specific competition for food in a pelagic seabird. *Nature* 412:816–819.
- Lynch, H. J., R. Naveen, P. N. Trathan, and W. F. Fagan. 2012. Spatially integrated assessments reveal widespread changes in penguin populations on the Antarctic Peninsula. *Ecology* 93:1367–1377.
- Martínez del Río, C., N. Wolf, S. A. Carleton, and L. Z. Gannes. 2009. Isotopic ecology ten years after a call for more laboratory experiments. *Biological Reviews* 84:91–111.
- Masello, J. F., R. Mundry, M. Poisbleau, L. Demongin, C. C. Voigt, M. Wikelski, and P. Quillfeldt. 2010. Diving seabirds share foraging space and time within and among species. *Ecosphere* 1:19.
- McMahon, K. W., L. L. Hamady, and S. R. Thorrold. 2013. A review of ecogeochemistry approaches to estimating movements of marine animals. *Limnology and Oceanography* 58:697–714.
- Newsome, S. D., C. Martínez del Río, S. Bearhop, and D. L. Phillips. 2007. A niche for isotopic ecology. *Frontiers in Ecology and the Environment* 5:429–436.
- Phillips, R. A., S. Bearhop, R. A. R. McGill, and D. A. Dawson. 2009. Stable isotopes reveal individual variation in migration strategies and habitat preferences in a suite of seabirds during the nonbreeding period. *Oecologia* 160:795–806.
- Phillips, R. A., J. R. D. Silk, J. P. Croxall, V. Afanasyev, and D. R. Briggs. 2004. Accuracy of geolocation estimates for flying seabirds. *Marine Ecology Progress Series* 266:265–272.
- Polito, M. J., H. J. Lynch, R. Naveen, and S. D. Emslie. 2011a. Stable isotopes reveal regional heterogeneity in the pre-breeding distributions and diets of sympatrically breeding *Pygoscelis* spp. penguins. *Marine Ecology Progress Series* 421:265–277.
- Polito, M. J., S. Abel, C. R. Tobias, and S. D. Emslie. 2011b. Dietary isotopic discrimination in gentoo penguin (*Pygoscelis papua*) feathers. *Polar Biology* 34:1057–1063.
- Polito, M. J., W. Z. Trivelpiece, W. P. Patterson, N. J. Karnovsky, C. S. Reiss, and S. D. Emslie. 2015. Contrasting specialist and generalist patterns facilitate foraging niche partitioning in sympatric populations of *Pygoscelis* penguins. *Marine Ecology Progress Series* 519:221–237.
- Quillfeldt, P., J. F. Masello, R. A. McGill, M. Adams, and R. W. Furness. 2010. Moving polewards in winter: A recent change in the migratory strategy of a pelagic seabird? *Frontiers in Zoology* 7:15.
- Quillfeldt, P., J. F. Masello, J. Navarro, and R. A. Phillips. 2012. Year-round distribution suggests spatial segregation of two small petrel species in

- the South Atlantic. *Journal of Biogeography* 40:430–441.
- R Core Team. 2012. R: A language and environment for statistical computing. R Foundation for Statistical Computing, Vienna, Austria.
- Ramos, R., and J. González-Solís. 2012. Trace me if you can: the use of intrinsic biogeochemical markers in marine top predators. *Frontiers in Ecology and the Environment* 10:258–266.
- Ratcliffe, N., S. Crofts, R. Brown, A. M. M. Baylis, S. Adlard, C. Horswill, H. Venables, P. Taylor, P. N. Trathan, and I. J. Staniland. 2014. Love thy neighbor or opposites attract? Patterns of spatial segregation and association among crested penguin populations during winter. *Journal of Biogeography* 41:1183–1192.
- Reynolds, R. W., N. A. Rayner, T. M. Smith, D. C. Stokes, and W. Wang. 2002. An improved in situ and satellite SST analysis for climate. *Journal of Climate* 15:1609–1625.
- Ricklefs, R. E. 1967. A graphical method of fitting equations to growth curves. *Ecology* 48:978–983.
- Ricklefs, R. E., and G. L. Miller. 1999. *Ecology*. Fourth edition. W.H. Freeman, New York, New York, USA.
- SAS Institute. 1999. SAS/GRAPH software: reference. Version 8. SAS Institute, Cary, North Carolina, USA.
- Schoener, T. W. 1970. Non-synchronous spatial overlap of lizards in patchy habitats. *Ecology* 51:408–418.
- Seminoff, J. A., S. R. Benson, K. E. Arthur, T. Eguchi, P. H. Dutton, R. F. Tapilatu, and B. N. Popp. 2012. Stable isotope tracking of endangered sea turtles: validation with satellite telemetry and $\delta^{15}\text{N}$ analysis of amino acids. *PLoS ONE* 7:e37403.
- Shaffer, S. A., Y. Tremblay, H. Weimerskirch, D. Scott, D. R. Thompson, P. M. Sagar, H. Moller, G. A. Taylor, D. G. Foley, B. A. Block, and D. P. Costa. 2006. Migratory shearwaters integrate oceanic resources across the Pacific Ocean in an endless summer. *Proceedings of the National Academy of Sciences USA* 103:12799–12802.
- Thiebot, J.-B., Y. Cherel, P. N. Trathan, and C.-A. Bost. 2011. Inter-population segregation in wintering areas of macaroni penguins. *Marine Ecology Progress Series* 421:279–290.
- Thiebot, J.-B., Y. Cherel, P. N. Trathan, and C.-A. Bost. 2012. Coexistence of oceanic predators on wintering areas explained by population-scale foraging segregation in space or time. *Ecology* 93:122–130.
- Trivelpiece, W. Z., S. Buckelew, C. S. Reiss, and S. G. Trivelpiece. 2007. The overwinter distribution of chinstrap penguins from two breeding sites in the South Shetland Islands of Antarctica. *Polar Biology* 30:1231–1237.
- Trivelpiece, W. Z., J. T. Hinke, A. K. Miller, C. S. Reiss, S. G. Trivelpiece, and G. M. Watters. 2011. Variability in krill biomass links harvesting and climate warming to penguin population changes in Antarctica. *Proceedings of the National Academy of Sciences USA* 108:7625–7628.
- Wilson, R. P. 2010. Resource partitioning and niche hyper-volume overlap in free-living Pygoscelid penguins. *Functional Ecology* 24:646–657.
- Wilson, R. P., B. M. Culik, P. Kosiorek, and D. Adelung. 1998. The overwinter movement of a chinstrap penguin (*Pygoscelis antarctica*). *Polar Record* 34:107–112.
- Wilson, R. P., J. J. Ducamp, G. Rees, B. M. Culik, and K. Niekamp K. 1992. Estimation of location: global coverage sun light intensity. Pages 131–143 in I. M. Priede and S. M. Swift, editors. *Wildlife telemetry: remote monitoring and tracking of animals*. Ellis Horward, Chichester, UK.

SUPPLEMENTAL MATERIAL

APPENDIX A

Summary of methods and results for the estimation of bias and error in GLS data

Estimating error (bias and precision) in location estimates is central to any animal tracking study. A basic approach for such analyses includes the deployment of control tags to

provide coordinates for known locations over time that can be used estimate bias corrections for raw data and provide estimates of precision for input into state-space models that are used to estimate migratory tracks of study animals. As part of our research using light-based geolocation tags (GLS) to study overwinter dispersal of Antarctic fur seals and penguins from two long-

Table A1. Summary information for four GLS tags used as stationary and mobile controls for estimation of error (bias and precision) in location. Numbers reported in the table represent the number of days. Daily location estimates were excluded if the GLS data were corrupt based on latitude error ($>90^\circ$ N or S or any northern hemisphere location), longitude error ($>180^\circ$ W or E), too distant from valid positions based on speed filtering, or because no overlapping ARGOS position estimate was available for mobile control tags. Note that the final number of days included for each tag span the date range specified.

Type	Original days in record	No. days lost to:				Final days in record	Final date range	Year
		Latitude errors	Longitude errors	Speed errors	No overlap with ARGOS			
Stationary	282	65	0	31	NA	186	27 Feb to 23 Nov	2011
Stationary	84	1	0	23	NA	60	3 Dec to 16 Feb	2011/12
Mobile	184	102	7	54	1	20	3 Mar to 6 July	2011
Mobile	112	29	0	35	6	42	3 Mar to 5 Jun	2011

term monitoring sites in the South Shetland Islands, we deployed two GLS tags (Lotek Nano-Lat 2900-series archival geolocation tags) on a stationary platform at Cape Shirreff, Livingston Island (62.4624° S, 60.7916° W) during the winters of 2011 and 2012 to monitor location estimation error at a fixed location. We also deployed 2 GLS tags on Antarctic fur seals already instrumented with SPOT5 satellite tags that were tracked via the ARGOS system during the winter for 2011. These mobile “control” tags were used to monitor error in GLS location estimates across a range of southern hemisphere latitudes and to assess whether bias and precision in the GLS data were independent of location.

For the purposes of the analysis using the mobile control tags, we assumed that a mean daily locations from ARGOS positions, calculated from all unique coordinates that had location quality codes 3 through A, provided sufficient precision to be classified as a known location with respect to the lower precision (~ 180 km) inherent in light-based geolocation estimates (Phillips et al. 2004). We also note that the four control tags were from different product batches, but onboard algorithms for estimating position were identical in all tags (P. O’Flaherty, *personal communication*).

Due to GLS tag failures during deployment, known errors in GLS location estimates during equinox periods (Wilson et al. 1992), impossible location estimates that were reported by the tags (latitudes $>90^\circ$ N or S and/or longitudes beyond 180° W or E), highly unlikely location estimates (any northern hemisphere locations), data points

deemed impossible based on a speed filter (Freitas et al. 2008), and a loss of potential data points due to non-overlap of ARGOS and GLS positions estimates for mobile controls, only 46% of the original daily coverage provided by the GLS data was available for this analysis (Table A1). Note that we used a maximum sustained speed of $3 \text{ m}\cdot\text{s}^{-1}$ to filter the control tag data for impossible points. This relatively high speed was used to retain as many data points as possible from the limited availability of control tag data. After filtering, the data set contained at least one (5.36 ± 3.2 ; mean \pm SD) location estimate for all weeks of the year except for week 8 (19 Feb–25 Feb), 13 (26 Mar–1 Apr), 30 (23 Jul–29 Jul), and 37–38 (10 Sep–23 Sep) when no GLS estimates of position were available.

Bias estimation

For each available location estimate from the GLS tags, we calculated the distance to its corresponding known daily location along latitude and longitude lines. These daily estimates of bias were then aggregated by week to calculate a weekly mean bias from the corresponding known location. We acknowledge that mobile tags may have extensive movement during the course of one week, but limited data availability from the mobile tags necessitated this aggregation. With the weekly mean latitudinal and longitudinal bias from each tag, we calculated a weekly weighted-average bias across all tags, with the weighting based on the number of daily location estimates contributed by each tag. This time series of weighted averages was then fitted with a smoothing spline to estimate the weekly

Table A2. Estimates of weekly bias and precision (in parentheses), measured in km, for latitude and longitude derived from control GLS data.

Week	Latitude	Longitude
1	-64.95 (39.97)	-40.54 (111.83)
2	-51.34 (56.86)	-48.58 (104.57)
3	-44.45 (75.06)	-51.13 (99.33)
4	-44.37 (94.07)	-48.82 (95.9)
5	-53.06 (112.59)	-43.24 (93.88)
6	-68.9 (130.29)	-33.92 (93.4)
7	-90.26 (147.25)	-16.94 (92.88)
8	-116.7 (164.33)	7.33 (93.19)
9	-164.59 (179.26)	24.38 (95.97)
10	-261.94 (195.89)	35.33 (100.06)
11	-377.99 (204.13)	28.42 (111.83)
12	-488.71 (207.23)	16.8 (129.16)
13	-566.93 (205.69)	0.76 (146.04)
14	-628.57 (200)	-15.41 (156.43)
15	-636.56 (193.82)	-19.59 (162.41)
16	-617.56 (184.54)	-21.61 (165.14)
17	-524.89 (151.51)	-20.08 (151.98)
18	-458.3 (122.33)	-10.98 (139.31)
19	-397.71 (98.86)	-2.25 (126.11)
20	-400.31 (93.31)	-7.75 (120.2)
21	-387.53 (109.29)	-17.61 (120.71)
22	-378.08 (128.28)	-28.41 (119.38)
23	-351.72 (140.39)	-34.2 (108.13)
24	-333.38 (143.29)	-39.58 (94.27)
25	-323.12 (143.99)	-43.84 (80.65)
26	-332.54 (141.34)	-51.07 (67.19)
27	-362.32 (134.92)	-46.04 (55.12)
28	-401.1 (121.24)	-37.44 (51.64)
29	-446.83 (114.81)	-25.34 (50.85)
30	-488.56 (110.7)	-13 (52.69)
31	-535.23 (108.45)	1.63 (51.78)
32	-586.49 (106.16)	10.68 (46.13)
33	-685.1 (106.8)	14.06 (40.31)
34	-720.2 (109.17)	9.5 (34.28)
35	-726.69 (110.32)	2.65 (30.74)
36	-671.69 (111.73)	-7.36 (27.53)
37	-567.39 (107.77)	-9.13 (27.34)
38	-404.76 (100.08)	-8.15 (28.7)
39	-236.98 (91.45)	-6.56 (32.37)
40	-117.25 (84.64)	-6.52 (39.15)
41	-38.26 (79.16)	-5.16 (50.34)
42	-16.2 (74.89)	-7.3 (63.08)
43	-19.46 (72.52)	-11.21 (76.58)
44	-28.12 (70.23)	-24.88 (91.28)
45	-19.56 (68.74)	-35.75 (106.49)
46	-12.99 (71.26)	-46.66 (121.85)
47	-18.42 (72.29)	-53.14 (134.16)
48	-26.48 (73.16)	-58.22 (145.31)
49	-38.05 (70.86)	-60.26 (156.19)
50	-52.01 (65.24)	-57.86 (166.83)
51	-69.23 (56.72)	-51.06 (177.25)
52	-89.74 (45.64)	-40.4 (187.3)

bias during the full year, including the 5 weeks with missing data. We used a loess smoother, implemented in R (R Core Team 2012), with span = 0.3 and degree = 2.0. The weekly estimates of latitudinal and longitudinal bias from the smoothing spline were then used to correct the

raw GLS data from all tracked animals.

The control-tag data identified a strong bias in latitude estimates during the austral winter, with GLS location estimates typically 400–600 km further north than known locations (Table A2, Fig. A1). The latitude bias was much reduced during the austral summer, with GLS location estimates typically within 200 km of known locations. Bias in longitude was smaller (generally <100 km) than for latitude, and exhibited no seasonal cycle (Table A2, Fig. A1).

Precision estimation

To estimate precision in the GLS locations, we used a two-step approach. First, we calculated a weighted variance, as described above for the weekly bias estimation, for the weekly estimates of latitudinal and longitudinal bias to represent the uncertainty in the raw GLS estimates of location. Second, we included uncertainty in position estimates introduced as a result of the bias correction by implementing a bootstrap approach. For the bootstrap procedure, we pooled the raw location estimates from all tags, randomly sub-sampled 75% of pooled data, reassigned the resulting data back to their respective tags, and repeated the weekly bias correction estimation procedure for the each tag outlined above. We repeated this process 10000 times (Fig. A3). From the resulting collection of smoothed bias corrections, we calculated the variance in the bias correction for latitude and longitude for each week. The variances estimated in steps 1 and 2 were added to estimate the total variance, and a square root was taken to estimate the weekly standard deviation of location precision. We then fitted a smoothing spline to the time series of standard deviations of location errors as a final estimate of weekly error in latitude and longitude position estimates for all weeks of the year, including those where no data were available.

The weekly estimates of error in latitude suggested that, on average, latitude error was roughly 1–2° (~111–222 km) while longitude error mainly ranged from 1° to 3° (~55–166 km) at these southern locales (assuming a latitude of 60° S). We used these upper bounds on latitude (2°) and longitude error (3°) to define grid cell sizes for mapping habitat utilization.

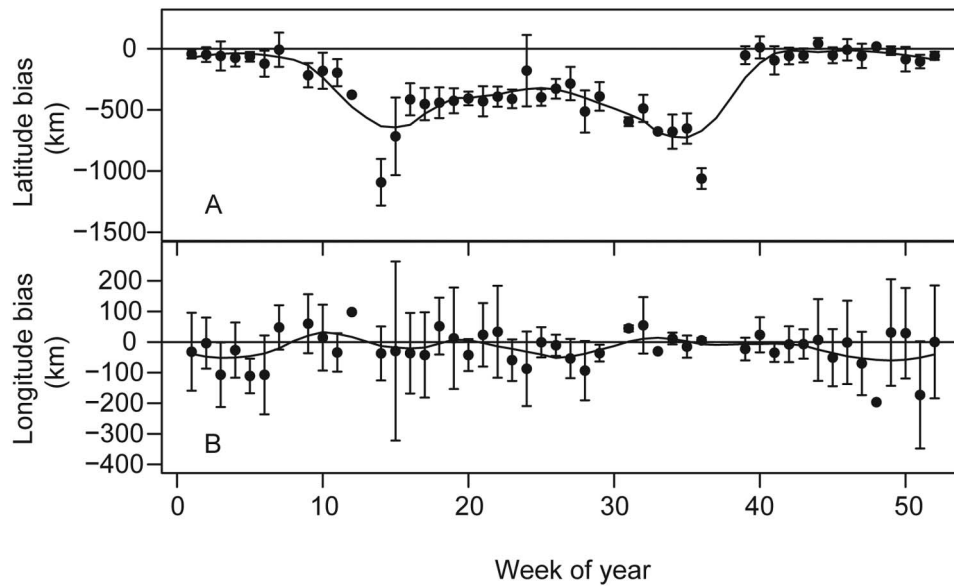


Fig. A1. Latitudinal (A) and longitudinal (B) bias (known location – GLS location), measured in km, for each week of the year. A smoothing spline is fitted to the data to estimate bias for weeks with missing data. Error bars represent weighted standard deviations of the weighted weekly means.

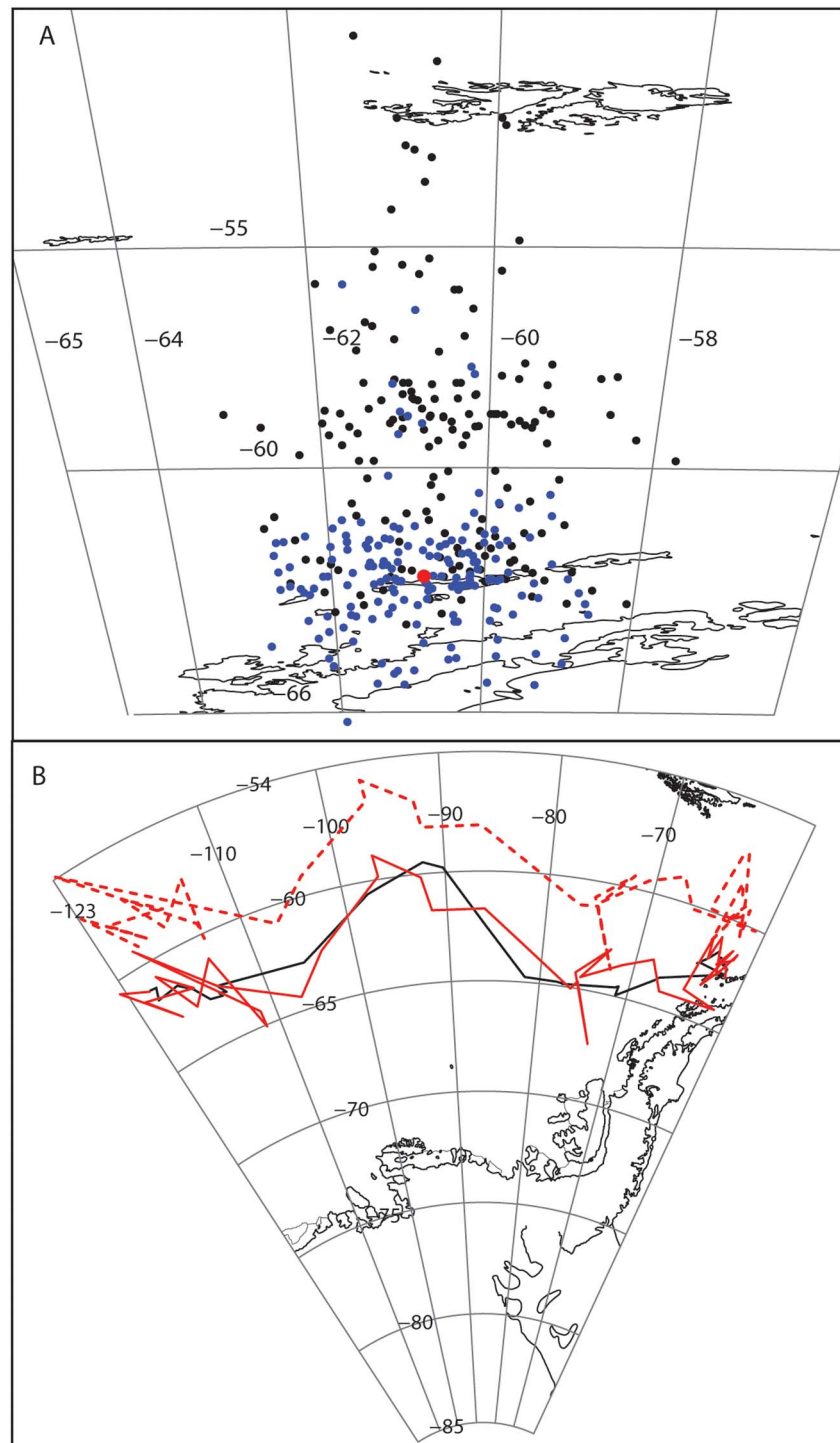


Fig. A2. Example of bias-corrected data for a stationary tag (A) and a mobile tag (B). (A) Raw GLS position estimates (black dots), known location at Cape Shirreff, Livingston Island (red dot), and bias corrected location estimates (blue dots). (B) ARGOS track line (solid black line), raw GLS track line (dashed red line) and bias-corrected GLS track line (solid red line) for mobile GLS tag 0588.

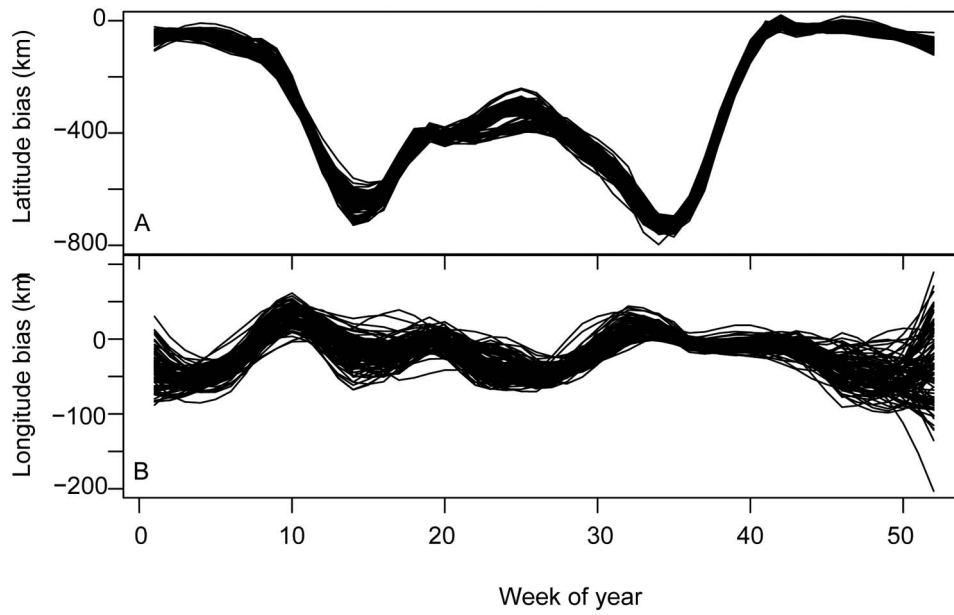


Fig. A3. Example plot showing 2000 iterations of the bootstrapping procedure to estimate variance in latitude (A) and longitude (B) due to the bias-correction procedure.

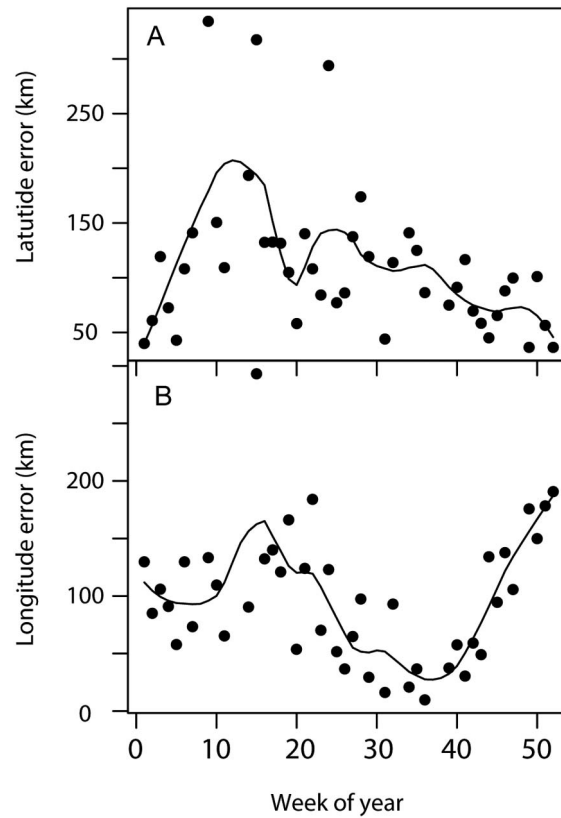


Fig. A4. Weekly error estimates for latitude (A) and longitude (B) and smoothed predictions (solid line). We used the smooth predictions for input into state-space models described in the main text and listed in Table A2.

APPENDIX B

Estimating the timing of tail-feather growth

We studied the growth of tail feathers in a captive population of Adélie penguins maintained at SeaWorld in Orlando, Florida, during 2012. To estimate the timing and rate of feather growth, twelve individual adults (6 male and 6 females) were monitored from the start of molt when flippers swell in size and old feathers begin to lift and stand out from the body. Following the onset of molt, the exposed length (cm) of the largest newly growing central tail feather of each individual was measured at roughly 20-day intervals until approximately 100 days after molt when growth of the tail feathers neared completion. We assume that rate of feather synthesis and, hence, the duration of the feather growth period, is similar between captive and wild animals. In support of this assumption we measured the exposed tail feather lengths in 122 wild (King George and Livingston Islands, South Shetland Islands) and 44 captive (SeaWorld) *Pygoscelis* penguins. Exposed tail feather did not differ across all wild and captive species either following body molt completion (ANOVA: $F_{3,71} = 0.79$, $P = 0.50$) when all feathers except the tail feathers are fully grown, nor outside of the molting period when tail feather are fully grown (ANOVA: $F_{4,93} = 2.30$, $P = 0.07$; Table B1). In addition, the duration of the body molt period is similar between wild and captive *Pygoscelis* penguins (Adams and Brown 1990, Polito et al. 2011b).

We note that the exposed length measurement does not account for the portion of each tail feather found beneath the skin. To address this difference, we measured both the exposed length and total length of plucked tail feathers from a sample of 19 Adélie (7 male and 12 female) and

33 chinstrap (19 male and 14 female) penguins instrumented with GLS tags at King George and Livingston Islands, South Shetland Islands. Mean hidden length (i.e., beneath the skin) of central tail feathers did not differ between species ($F_{1,52} = 0.174$, $P = 0.678$), sexes ($F_{1,52} = 0.1324$, $P = 0.572$) or exhibit a significant interaction ($F_{1,52} = 0.188$, $P = 0.666$). Therefore we added the overall mean hidden length (3.2 cm) across all species and sexes to our measurements of exposed tail feather length and derived the total length of growing tail feathers measured in our captive study (Table B1). We then used PROC NLIN with the Marquardt method in SAS (SAS Institute 1999) to fit von Bertalanffy growth curves to this dataset. The von Bertalanffy growth curve has been commonly used to model growth in large seabirds (Ricklefs 1967) and is formulated as:

$$L_t = t_\infty \left(1 - e^{-k(t-t_0)} \right)$$

where L_t is the predicted length (in cm) at time t (in days), L_∞ is the mean length that would be reached if feathers grew indefinitely, k is a growth parameter of dimension time^{-1} , and t_0 is the hypothetical time (in days) when feather length is zero. We modeled growth curves separately by sex and with both sexes combined and compared 95% confidence intervals of parameter estimates, residual mean square error (MSE) and pseudo- R^2 as measures of goodness of fit. Both MSE and pseudo- R^2 indicated that the von Bertalanffy growth curve fitted our data for males slightly better than for females and both sexes combined, though 95% confidence intervals (CI) of parameter estimates overlapped substantially between all three models (Table B2). Due to this overlap and the relatively small differences between sexes we used the parameter estimates derived from both sexes combined to estimate

Table B1. Comparison of exposed tail feather length immediately after the body molt is complete and outside of the molt period in wild and captive penguins.

Group	Species	Exposed tail feather at body molt completion		Exposed fully grown tail feather	
		<i>n</i>	Length (cm)	<i>n</i>	Length (cm)
Wild	Adélie	18	15.5 ± 1.2
	Chinstrap	20	2.0 ± 0.7	34	14.6 ± 1.2
	Gentoo	30	2.4 ± 0.9	20	14.9 ± 1.0
Captive	Adélie	12	2.0 ± 1.0	12	14.9 ± 1.4
	Chinstrap
	Gentoo	10	2.2 ± 0.8	10	14.5 ± 1.2

Table B2. Parameter estimates, 95% confidence intervals (in parentheses), residual mean square error (MSE) and pseudo- R^2 values estimated from fitted von Bertalanffy growth equations of total feather length (cm) relative to time (days) elapsed since the onset of feather molt.

Group	Parameter estimates			Fit statistics	
	L_∞	k	t_0	MSE	Pseudo- R^2
Males	19.5 (18.0–21.1)	0.03 (0.02–0.04)	7.8 (4.8–10.8)	0.765	0.968
Female	18.3 (16.1–20.4)	0.03 (0.02–0.05)	8.2 (2.9–13.5)	2.6	0.877
Combined	18.8 (17.5–20.2)	0.03 (0.02–0.04)	8.0 (4.9–11.1)	1.766	0.918

Table B3. Molt-timing information based on opportunistic observations of individuals at study colonies. All data are unpublished US AMLR holdings.

Species	Date	Molt chronology	How	n
Chinstrap†	10 Feb (± 5 d)	Initiation	Observations of banded individuals molting	254
Chinstrap†	19–27 Feb	Completion	Animals selected for overwinter tracking must be fully molted for tag attachment	30
Adélie‡	10 Feb	Initiation	Observations of banded individuals molting	1
Adélie	28 Feb	Completion	Animals selected for overwinter tracking must be fully molted for tag attachment	3
Adélie	11 Feb–11 Mar	Initiation	Loss of telemetry data due to presumed molt	4

† The opportunistically collected data on chinstraps reported here likely reflect timing for non-breeders and failed breeders and may be atypical of successful breeders. When annual research activities at Cape Shirreff end, typically in late February and early March, aggregations of molting birds are still growing. Thus, we assume 1 March to be a more representative molt initiation date for the majority of breeders despite the observational data suggesting otherwise.

‡ Observations of Adélie penguins molting on land in Admiralty Bay are rare.

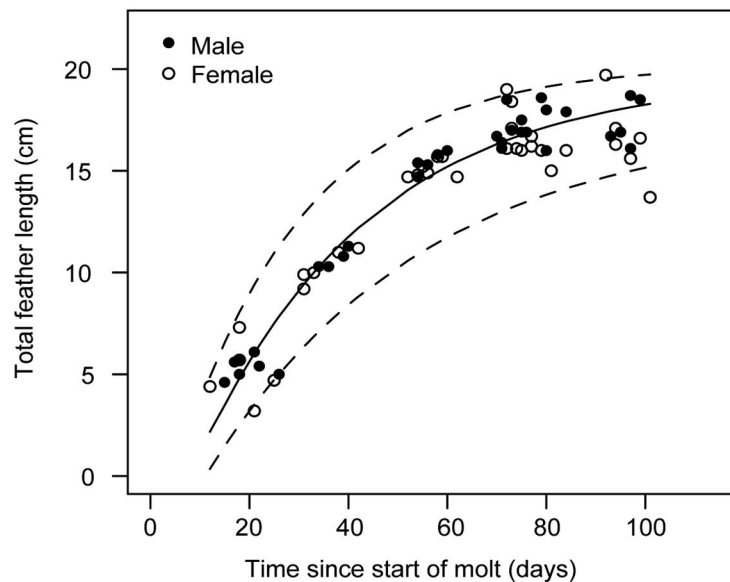


Fig. B1. Fitted von Bertalanffy growth curve (solid line) and 95% confidence intervals (dotted lines) of total tail feather length relative to time elapsed since the onset of feather molt in a captive population of twelve adult (6 male and 6 females) Adélie penguins maintained at SeaWorld in Orlando, Florida, during 2012.

the timing of tail feather synthesis based on length (Fig. B1):

$$t = t_0 - \frac{1}{k} \times \ln\left(1 - \frac{L_t}{L_\infty}\right)$$

where t is the predicted time (in days) since the start of molt that a section of tail feather at length L_t was synthesized based on the predicted von Bertalanffy growth parameters ($L_\infty = 18.832$, $k = 0.031$, $t_0 = 8.035$).

We applied the above formula to estimate timing of growth for discrete sections of tail feathers that were obtained from individual penguins tracked with GLS instruments. Discrete sections of the tail feathers were sampled for stable isotope analysis by using stainless steel scissors to cut a 0.5-cm section of feather shaft

from the proximal portion of each feather located just above where the feather enters the skin. These mid-point of each section average 15.6 ± 1.1 and 14.9 ± 1.3 cm from the distal tip and thus represented growth occurring 69 ± 20 (CI = 42–110) and 59 ± 11 (CI = 40–96) days following the onset of molt for Adélie and chinstrap penguins, respectively (i.e., 40–100 days following the onset of molt). Given published (Dunn et al. 2011) and unpublished data on molt timing (Table B3) for Adélie and chinstrap penguins, we assume that molt initiation typically occurred on 14 February for Adélie penguins and 1 March for chinstrap penguins. Thus, the sampled feather sections reflect a time from late March to early June when penguins are migrating to and/or inhabiting their over-wintering areas.

APPENDIX C

Monthly habitat utilization and distributions of surface temperature readings measured by GLS tags deployed on chinstrap and Adélie penguins (see following pages)

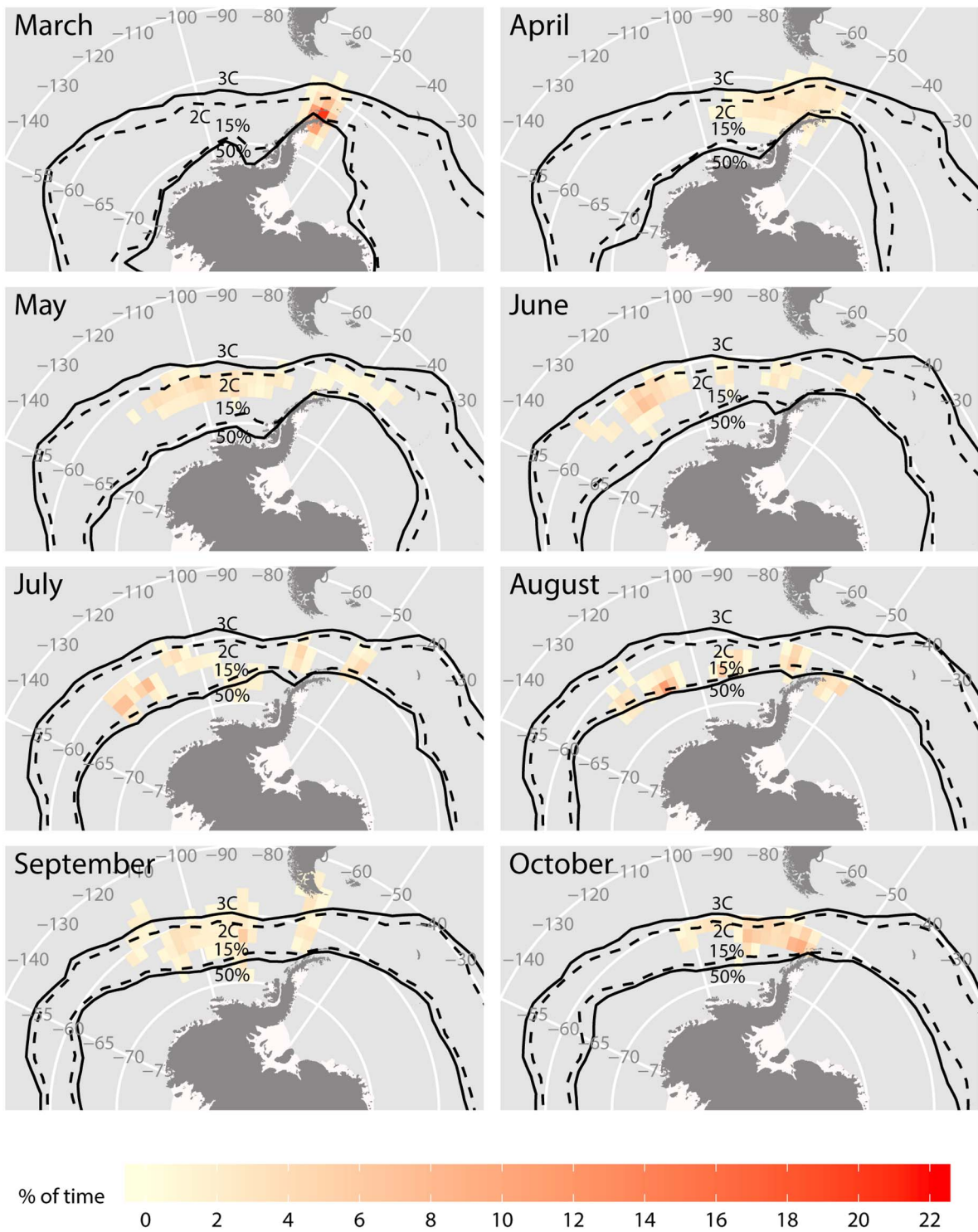


Fig. C1. Monthly habitat utilization for chinstrap penguins during the non-breeding season.

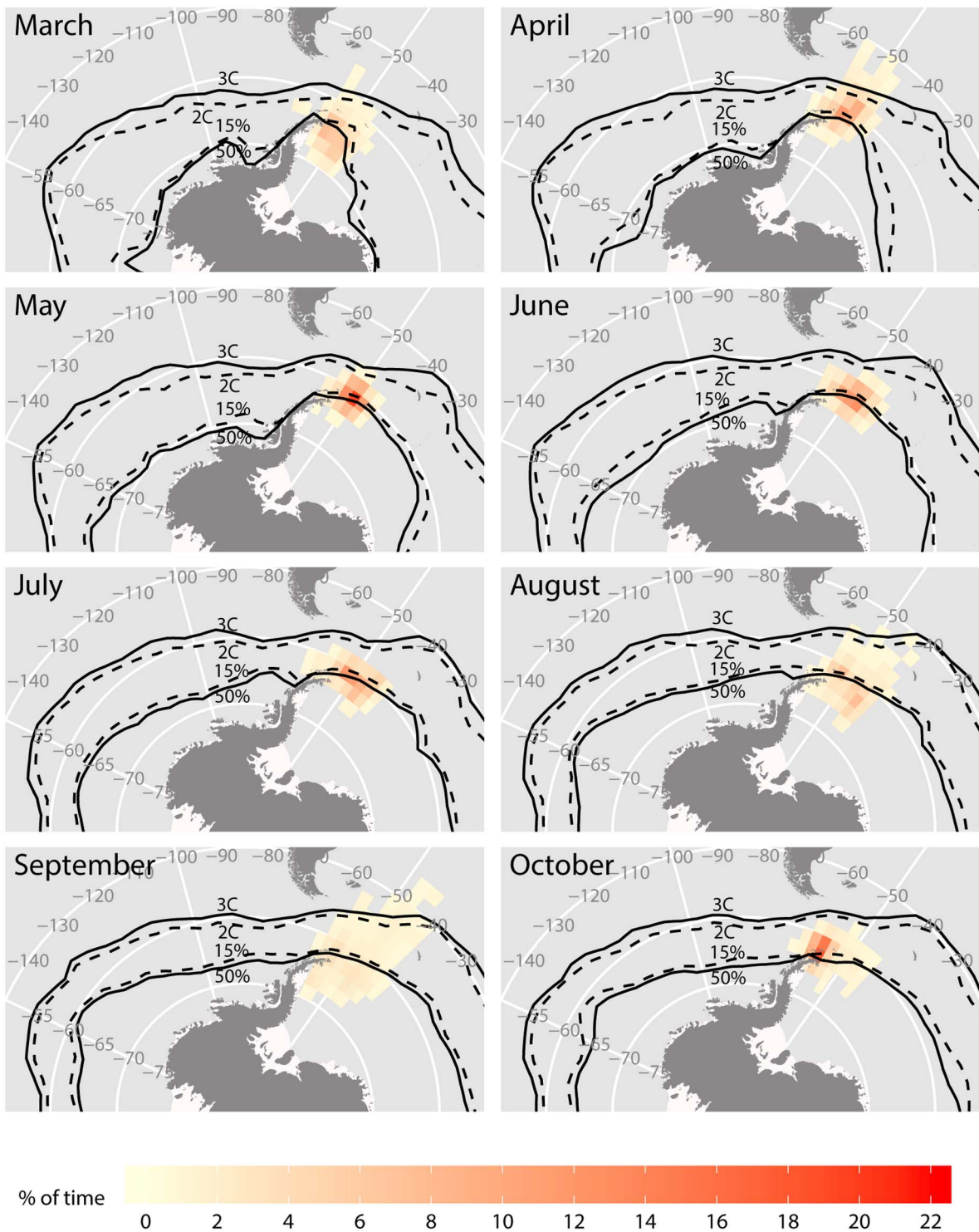


Fig. C2. Monthly habitat utilization for Adélie penguins during the non-breeding seasons.

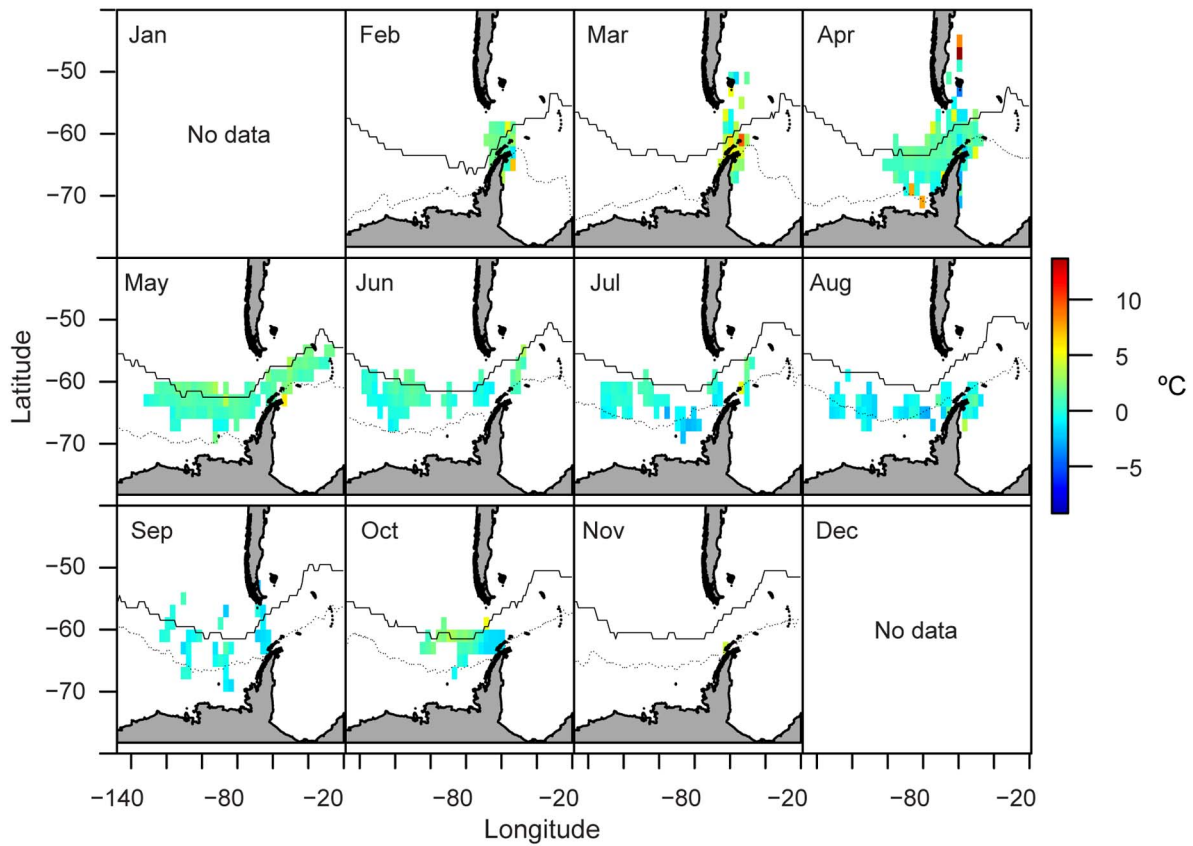


Fig. C3. Monthly surface temperature distributions for chinstrap penguins. Data derive from once-daily records of surface temperatures recorded by GLS tags, averaged over each month for each grid cell. Position estimates used for this plot are bias-corrected, raw data.

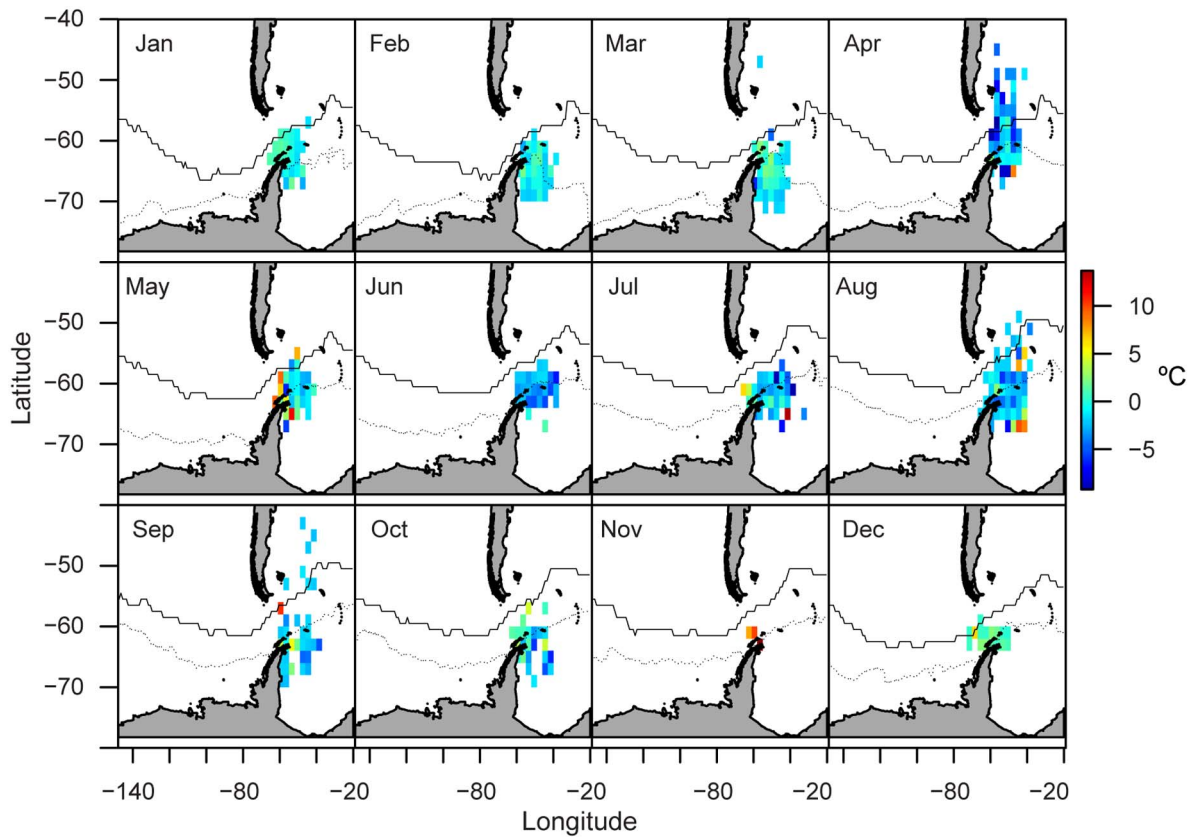


Fig. C4. Monthly surface temperature distributions for Adélie penguins. Data derive from once-daily records of surface temperatures recorded by GLS tags, averaged over each month for each grid cell. Position estimates used for this plot are bias-corrected, raw data.